

國立交通大學

應用化學系

碩士論文

結合連續波與飛秒脈衝雷射在時間與空間上控制甘
胺酸單一結晶的形成

Spatial-temporally controlled single crystal formation of glycine by a
combination of continuous wave and femtosecond pulse lasers

研究生：黃彥樺

指導教授：增原 宏 教授

中華民國一百零一年七月

結合連續波與飛秒脈衝雷射在時間與空間上控制甘
胺酸單一結晶的形成

Spatial-temporally controlled single crystal formation of glycine by a
combination of continuouswave and femtosecond pulse lasers

研 究 生：黃彥樺

Student：Yan-Hua HUANG

指 導 教 授：增原宏 博士

Advisor：Dr. Hiroshi MASUHARA



A Thesis
Submitted to M. S. Program
Department of Applied Chemistry
National Chiao Tung University
in Partial Fulfillment of the Requirements
for the Degree of
Master
in
Applied Chemistry

July 2012

Hsinchu, Taiwan, Republic of China

中華民國一百零一年七月

Spatial-temporally controlled single crystal formation of glycine by a combination of continuouswave and femtosecond pulse lasers

Student : Yan-Hua HUANG

Advisor : Dr. Hiroshi MASUHARA

M. S. Program, Department of Applied Chemistry
National Chiao Tung University

Abstract

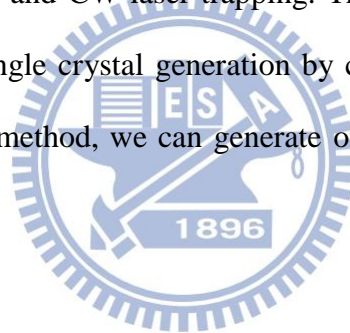
Light irradiation-induced crystallization is attracting much attention as novel phenomena and as potential methods to control single crystal formation. It has been reported that focusing of an amplified fs pulse ($\mu\text{J} \sim \text{mJ}/\text{pulse}$) into a supersaturated solution induces the bubbling due to fs laser-induced break-down of water and eventual crystallization and CW laser trapping with saturated solution induces local concentration increase and spatially controlled crystallization. Recent report on fs laser trapping of particles stimulating us to use fs pulses to improve laser trapping crystallization technique. We can expect higher crystallization efficiency with higher photon density of fs laser in a short time compare to CW laser. Thus here we report first demonstration of low energy fs pulse utilized laser trapping crystallization of glycine without conventional bubbling.

Glycine/D₂O solution (2.4~2.6 M, supersaturation degree: 0.9~1.0) was prepared and a portion of the solution was dropped in a sealed glass sample chamber to form a thin liquid layer ($\sim 120 \mu\text{m}$). An output from Ti:sapphire laser ($\lambda=800 \text{ nm}$), which can be operated with pulse (80 MHz, 150 fs) and CW modes, was focused to the air/solution interface through an objective lens (60X, NA 0.90).

We observed crystal generation from a focal spot of fs laser. Laser fluence threshold of

crystallization is below than that of the bubbling. No bubbling and no other apparent nonlinear behavior was observed during crystallization. Crystallization was effectively induced compared to 800 nm CW laser utilized trapping crystallization. We consider that repetitively exerted photon pressure induced by irradiated fs laser pulse collects molecules, forms high concentration area locally around the laser spot, and induces fluctuation and re-orientation of the clusters, leading to crystallization.

However frequently observed fs laser ablation on generated crystal resulted in polycrystal formation. Thus we need to improve the crystallization method to make the application of femtosecond laser in single crystal formation. We have examined a single crystal generation which was induced by fs only or a fs/CW combination. Finally we succeeded to make single crystal by a combination of fs and CW laser trapping. The most important achievement in this study is the success of single crystal generation by combining short fs irradiation and CW laser irradiation. By this method, we can generate one single crystal with high spatial and temporal controllability.



結合連續波與飛秒脈衝雷射在時間與空間上控制甘胺酸單一結晶的形成

研究生：黃彥樺

指導教授：增原宏 博士

國立交通大學 應用化學系碩士班

中文摘要

光線照射誘導結晶，作為新的現象和潛在的控制單晶形成方法，吸引了研究者的高度重視。文獻指出增幅脈衝雷射在過飽和溶液中誘發水分解，而產生冒泡導致結晶；和連續波雷射捕陷於飽和溶液中，誘發局部高濃度並於空間上控制結晶化。近來的飛秒脈衝雷射捕陷分子研究，促使我們使用飛秒雷射來改善雷射捕陷結晶化技術。相較連續波雷射，飛秒脈衝雷射在單一脈衝的時間內有更高的光子數，因此我們可以期待飛秒雷射可以帶來更好的結晶效率。這裡我們第一個示範以低能量飛秒脈衝雷射執行雷射捕陷結晶化，並且過程中沒有觀察到冒泡現象。

甘胺酸重水溶液(2.4~2.6 M，飽和度：0.9~1.0)滴入一個密封的玻璃容器並形成一個薄的液層(~120 μm)。Ti:sapphire 雷射($\lambda=800\text{ nm}$)可以控制輸出為脈衝(80 MHz, 150 fs)及連續波模式，此雷射光經由物鏡(60X, NA 0.90)聚焦到空氣與溶液的介面。

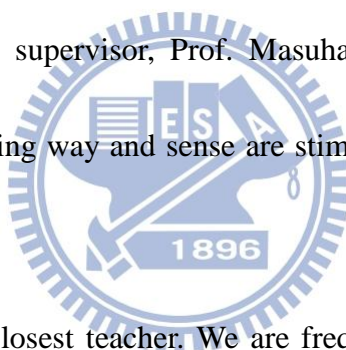
我們到在飛秒雷射的焦點上觀察到結晶的產生，結晶過程中並沒有觀察到冒泡及其他非線性光學現象，得知雷射誘發結晶的低限能低於冒泡的低限能。相較於同樣波長的連續波雷射捕陷結晶化技術，飛秒脈衝雷射誘發結晶是更有效率的，我們認為飛秒雷射以更強的光壓收集分子，在焦點形成局部高濃度，並誘導分子叢的變動及從新排列，進一步使結晶化產生。

然而，飛秒雷射能量太強，熔蝕了結晶，導致多核結晶的形成，因此我們必須改善結晶的方法使飛秒雷射應用於單一結晶的製備。我們驗證了只使用飛秒雷射的條件，或結合連續波與飛秒脈衝雷射，並在這些條件下成功的控制單一結晶的形成。最重要的方法是結合短時間的飛秒雷射照射，及長時間的連續波雷射照射，形成單一結晶，我們可以使用這個方法達成高度的時間及空間上的控制能力。

Acknowledgement

I feel very lucky that I had the chance to join this great group. I met many foreign peoples. We discussed, worked, and exchanged culture, shared nice experiences. During the study in this laboratory, I had a chance to visit Japan to learn experimental skill. That was my first time to go to an aboard. These experiences are so beautiful that I cannot forget forever. Life in this laboratory is really enjoyable and I thank everything here.

I have to appreciate to my supervisor, Prof. Masuhara. He kindly guided me in this laboratory. His scientific thinking way and sense are stimulating. I am very glad and proud that I can study with him.



Thank to Prof. Miura, the closest teacher. We are frequently discussing and contacting, even fighting with different viewpoints. Thanks to his kindness teaching, without that, I must not able to finish my study. I am very appreciating that we had such special relationship in this two years.

I also want to thank Prof. Sugiyama that he gives me lots useful suggestions. His great supporting let me breakthrough my blind spots of my research. Dr. Yuyama improves my understanding of my study and gives me helpful ideas. Dr. Usman teaches me a lot and helps me how to construct optical setup. Prof. Uwada gives me the suggestions for a positive

research attitude. I am very grateful for their help.

I must have to thanks my seniors and classmates: 許平諭, 杜靜如, 劉宗翰, 黃重維, 曾
祭續, 許孜瑋, 王順發, 江威逸, 黃鈴婷, 吳奇勳。Thanks for their companying with nice
atmosphere and encouragement to me when I was disappointed. Specially thanks to 許平諭,
杜靜如, 黃重維, they help me a lot for research and how to live in Hsinchu. Wish them will
get great achievement in the future.

Finally, sincerely thanks to my family and friends for their supporting and concerning and
support to finish master degree.



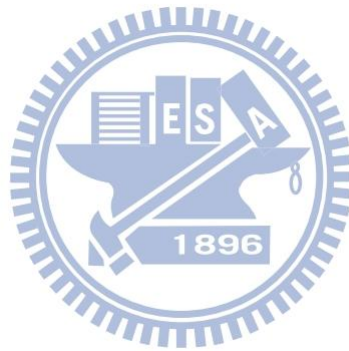
Table of Contents

| | |
|--|------|
| Abstract | iii |
| 中文摘要 | v |
| Acknowledgement..... | vi |
| Table of Contents | viii |
| List of Figures | xi |
| List of Tables..... | xv |
| 1. Introduction | 1 |
| 1.1 Laser trapping..... | 1 |
| 1.1.1 History of laser trapping..... | 1 |
| 1.1.2 Principle of laser trapping | 2 |
| 1.1.3 Laser trapping-induced assembly formation..... | 5 |
| 1.1.4 Laser trapping by applying pulse laser..... | 8 |
| 1.2 Crystallization | 9 |
| 1.2.1 History of biomolecular crystallization..... | 10 |
| 1.2.2 Crystallization theory | 11 |
| 1.3 Light-induced crystallization methods | 14 |
| 1.3.1 Kerr effect crystallization..... | 14 |
| 1.3.2 Photochemical reaction-induced crystallization..... | 15 |
| 1.3.3 Amplified femtosecond laser-induced crystallization..... | 16 |
| 1.3.4 Laser trapping crystallization | 17 |
| 1.4 Motivation | 18 |
| 2. Experiment | 20 |
| 2.1 Materials..... | 20 |
| 2.2 Property of glycine | 22 |
| 2.3 Laser mode | 25 |

| | | |
|-------|--|----|
| 2.3.1 | Continuous wave laser light source..... | 26 |
| 2.3.2 | Femtosecond laser light source | 27 |
| 2.4 | Microscope setup for imaging of crystallization behavior | 28 |
| 2.5 | Fourier transfer infrared spectra measurement..... | 29 |
| 3. | Continuous Wave Laser-Induced Crystallization..... | 32 |
| 3.1 | Power dependence of laser trapping crystallization | 32 |
| 3.2 | Volume/Thickness dependence of laser trapping crystallization | 37 |
| 3.3 | Summary | 39 |
| 4. | Femtosecond Laser-Induced Crystallization..... | 40 |
| 4.1 | Crystallization of glycine by femtosecond pulse laser | 40 |
| 4.2 | Power dependence on fs laser trapping crystallization..... | 43 |
| 4.3 | Focus position dependence on fs laser trapping crystallization | 44 |
| 4.4 | Comparison between fs and CW laser trapping crystallization..... | 45 |
| 4.5 | Discussion | 50 |
| 4.5.1 | Trapping by low energy fs laser operated at high repetition rate | 50 |
| 4.5.2 | Comparisons of fs laser trapping crystallization and amplified fs laser-induced crystallization | 52 |
| 4.5.3 | Comparisons of fs and CW trapping crystallization | 54 |
| 4.6 | Summary | 55 |
| 5. | Single crystal formation by a combination of fs and CW lasers | 56 |
| 5.1 | Femtosecond laser-induced crystallization: Approach 1, fs for nucleation and growth without laser irradiation..... | 56 |
| 5.2 | Femtosecond laser-induced crystallization with further CW laser irradiation | 60 |
| 5.3 | Low power CW laser trapping crystallization with a short time irradiation of fs laser..... | 63 |
| 5.4 | Temporal control of crystallization by millisecond exposure time of fs laser | 68 |
| 5.5 | FTIR measurements for generated glycine crystals | 72 |
| 5.6 | Summary | 75 |

6. Summary 77

7. Reference..... 79



List of Figures

| | | |
|----------|---|----|
| Fig. 1.1 | Ray diagram shows difference of the direction of gradient force (gray arrows) induced by unfocused (a) and focused (b) light. | 3 |
| Fig. 1.2 | Schematic drawing of the relationship between refractive indices of particle (n_1) and medium (n_2) and the direction of gradient force (F). | 4 |
| Fig. 1.3 | Schematic view of PNIPAM assembly via photon pressure and phase transition [12]. | 6 |
| Fig. 1.4 | Schematic picture of proposed transportation of nanoparticles due to the convection flow under the laser trapping in water. [20]. | 7 |
| Fig. 1.5 | Schematic drawing of classical nucleation theory, crystal growth by packing of molecules [34]. | 11 |
| Fig. 1.6 | Schematic illustration of the two-step mechanism of nucleation of crystals (dot line) [35]. | 12 |
| Fig. 1.7 | Free energy diagram for possible crystallization processes [34]. | 13 |
| Fig. 1.8 | Phase diagram showing the solubility depends on temperature and concentration. Once solution became highly saturated with higher free energy in the labile or metastable region, nucleation could take place, causing a reduction of free energy and the phase returned to the stable region. | 13 |
| Fig. 1.9 | Mechanism of (a) the photochemically induced nucleation of lysozyme, and (b) enhancement of protein crystallization by a photochemical reaction [44]. | 15 |
| Fig. 2.1 | Pictures of container made of (a) cut glass vial and (b) short glass tube. | 22 |
| Fig. 2.2 | Schematic drawing of surface shape: (a) cut glass vial and (b) short glass tube. | 22 |
| Fig. 2.3 | The chemical structure of glycine. | 23 |
| Fig. 2.4 | Schematic diagram of the morphology of the (a) α - and (b) γ -glycine single crystals [4]. | 24 |
| Fig. 2.5 | Picture of Nd:YVO ₄ laser, J20-BL10-106Q, used in this study. | 27 |
| Fig. 2.6 | Picture of (a) mode-locked Ti:sapphire laser, Tsunami and (b) pump laser, MillenniaPro. | 28 |
| Fig. 2.7 | Optical set up of laser-induced crystallization system. | 29 |
| Fig. 2.8 | A multiple reflection ATR system. Light undergoes multiple internal reflections in the ATR crystal of high refractive index, shown in yellow. The sample is in contact with the crystal. | 31 |
| Fig. 3.1 | Power dependence of laser trapping crystallization with a focused (a) CW 1064 nm and (b) CW 800 nm laser. Laser was focused to the air/solution interface of the glycine solution. Power of 200, 400, 600, and 800 mW CW laser was examined for 1064 nm with 1.0 SS solution; Power of 400 and 600 mW CW laser was examined | |

| | | |
|----------|--|----|
| | for 800 nm with 0.9 SS solution. The examined crystallization time is 30 minutes. | 33 |
| Fig. 3.2 | Images of glycine crystal generation and growth by CW laser trapping. Saturation degree is 0.9 SS. Laser power is 600 mW..... | 34 |
| Fig. 3.3 | Solution height change during 1064 nm CW laser irradiation in cover glass case, laser was focused to the air/solution interface of the thin glycine solution layer formed on the glass substrate. Above curve was obtained with 1.32 SS solution. Laser power is 1.0 W. Asterisk indicates the timing when crystallization occurred. | 36 |
| Fig. 3.4 | Solution height change during 1064 nm CW laser irradiation in cut glass vial case. Laser was focused to the air/solution interface of the glycine solution. Above curve was obtained with 1.0 SS solution. 200, 400, 600 mW laser power was examined. Cut glass vial was used as a container. Asterisk indicates crystallization occurred in 600 mW case. | 37 |
| Fig. 3.5 | Solution (a) volume and (b) thickness dependent crystallization time. Curves were obtained with 1.32 SS solution. Laser power is 1.0 W. Short glass tube was used as a container. | 38 |
| Fig. 3.6 | Solution thickness dependence on crystallization time. Curves were obtained with 1.32 SS solution. Laser power is 1.0 W. Short glass tube was used as a container. Asterisk indicates crystallization occurred. | 38 |
| Fig. 4.1 | Images taken during fs pulse laser induced trapping crystallization. Before fs laser irradiation (a), generated crystal (b), and trapped and grown crystal (c) and (d). Saturation degree of solution is 1.0 SS. Laser power is 600 mW. Similar to CW laser trapping crystallization, solution height did not change obviously but slightly decreased during fs laser irradiation to the air/solution interface. | 41 |
| Fig. 4.2 | Comparison of the solution height change under trapping laser irradiation. Both 1064 nm CW (blue line) and 800 nm fs (red line) lasers were set to the same average power (400 mW) and focused to the air/solution interface of the glycine solution. Asterisk indicates the moment crystallization occurred in 800 nm fs laser. Black dotted line in the figure is solution height change without laser irradiation. | 42 |
| Fig. 4.3 | Power dependence of crystallization time of fs laser trapping crystallization. 100, 200, 300, 400, and 600 mW fs laser was applied. Observation time is 30 min. Saturation degree of solution is 0.9 SS. | 43 |
| Fig. 4.4 | Focus position dependence on fs laser trapping crystallization. Crystallization occurred only focusing to the air/solution interface as well as CW laser trapping crystallization. Saturation degree of solution is 0.9 SS. Laser power is 600mW. ... | 45 |
| Fig. 4.5 | Snapshots of laser trapping crystallization process induced by (a) CW and (b) fs laser. Average laser power of both lasers were 600 mW. Saturation degree of | |

| | | |
|-----------|---|----|
| | solution is 0.9 SS..... | 47 |
| Fig. 4.6 | (a) Crystal pictures and crystal size definition, and (b) crystal growth rate by irradiating fs and CW lasers. Laser power is 600 mW. Saturation degree of the solution is 0.9 SS..... | 48 |
| Fig. 4.7 | (a) Crystallization probability and (b) crystallization time induced by fs and CW lasers. Green and red markers correspond to CW and fs laser, respectively. Examined laser powers are 100, 200, 300, 400, 600 mW. Saturation degree of the solution is 0.9 SS. Observation time is 30 min. | 48 |
| Fig. 4.8 | Pictures of (a) CW laser-induced single glycine crystal and (b) fs laser-induced polycrystal. In fs case, crystal growth and damage on the crystal surface simultaneously took place..... | 49 |
| Fig. 4.9 | Illustration of laser energy comparison of low energy fs laser, amplified fs laser, and CW laser. | 50 |
| Fig. 4.10 | Schematic drawing of femtosecond laser trapping induced accumulation of molecule at the focal spot..... | 52 |
| Fig. 4.11 | Schematic drawing of focused amplified fs laser and low energy fs laser focused into the solution. Micrometer-size cavitation bubble plays a key role in amplified fs laser. Supersaturated glycine solution is necessary in the amplified fs laser case. | 54 |
| Fig. 5.1 | (a) Sequential pictures obtained during fs laser trapping crystallization and crystal growth without laser irradiation and (b) schematic drawing of femtosecond laser-induced crystallization by terminating fs laser irradiation after observing crystal generation. fs laser power is 400 mW. Saturation degree of solution is 1.0 SS. | 57 |
| Fig. 5.2 | Schematic drawing of solvent evaporation process to obtain a millimeter-size crystal. | 58 |
| Fig. 5.3 | Pictures of the obtained millimeter-size single crystal of femtosecond laser-induced crystallization without further irradiation..... | 59 |
| Fig. 5.4 | Schematic drawing of dissolution of formed crystal in unsaturated region. Deep blue means the high concentration area induced by trapping laser..... | 60 |
| Fig. 5.5 | (a) Pictures of the crystallization and (b) schematic drawing of fs laser-induced crystallization with further CW laser irradiation. Power of both fs and CW laser is 400 mW. Saturation degree of solution is 1.0 SS..... | 61 |
| Fig. 5.6 | Pictures of the obtained millimeter-size single crystal of femtosecond laser-induced crystallization with further continuouswave laser irradiation. | 62 |
| Fig. 5.7 | Schematic drawing of low power CW laser trapping crystallization with a short time irradiation of fs laser. | 64 |
| Fig. 5.8 | (a) Schematic drawing of laser irradiation manner in simultaneous fs and CW laser | |

| | | |
|-----------|---|----|
| | irradiation. (b) Laser trapping crystallization of glycine by focusing 1064 nm cw and 800 nm fs laser simultaneously. The limited experiment time is 30 minutes. Saturation degree of solution is 1.0 SS. | 65 |
| Fig. 5.9 | (a) Schematic drawing of laser irradiation manner in method 3. (b) Success probability and crystallization time of low power CW laser trapping crystallization with a short time irradiation of fs laser. The red arrow means fs laser irradiated. The limited experiment time is 30 minutes. Saturation degree of solution is 1.0 SS. | 66 |
| Fig. 5.10 | Pictures of the crystallization of low power CW laser trapping crystallization with a short time irradiation of fs laser. | 67 |
| Fig. 5.11 | (a) Images and (b) schematic drawing of temporally controlled laser-induced crystallization by millisecond short time irradiation of fs laser. Power of fs and CW lasers are 200 and 400 mW, respectively. Saturation degree of solution is 1.0 SS. | 69 |
| Fig. 5.12 | Schematic mechanism of millisecond short time irradiation of fs laser induced crystallization. fs laser irradiation gathers the surrounding glycine cluster together. Suddenly concentration became high enough for crystallization. | 70 |
| Fig. 5.13 | Phase diagram showing the solubility depends on temperature and concentration. Suddenly fs laser irradiation induced highly saturated area in the labile region and finally persuaded nucleation and crystallization. | 71 |
| Fig. 5.14 | FTIR spectra of glycine crystals prepared by single crystal formation by combination of CW and fs laser. α - and γ -form spectra of glycine-d ₃ was obtained | 74 |

List of Tables

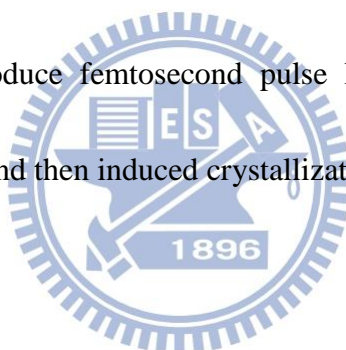
| | | |
|-----------|--|----|
| Table 2.1 | Solubility of glycine in H ₂ O and D ₂ O [2]..... | 23 |
| Table 4.1 | Crystallization probability and time for different trapping laser power of fs and CW laser trapping crystallization. | 47 |
| Table 5.1 | Setting fs laser irradiation time and crystallization probability under different combination of CW and fs lasers..... | 67 |
| Table 5.2 | Vibrational frequencies of <i>N</i> -deuterated glycine (ND ₃ ⁺ CH ₂ COO ⁻ , glycine-d ₃) | 74 |



1. Introduction

1.1 Laser trapping

Laser trapping is a powerful technique for controlling and manipulating particles in chemistry, biology and physics. This technology has offered a precise method for manipulating objects from a few tens of nanometer to tens of micrometer in size by using the optical gradient force. A continuous wave (CW) laser is usually used for the laser trapping, meanwhile we introduce femtosecond pulse laser for trapping molecules and forming molecular assembly, and then induced crystallization.



1.1.1 History of laser trapping

Arthur Ashkin is one of the pioneers of laser trapping. He and his colleagues were first demonstrated the optical trapping of transparent micron-sized particle in 1970 [1]. They observed that micron-sized particle in liquids or gas can be trapped by radiation pressure caused by exerted laser. Based on the basic scattering and gradient force of radiation pressure, the trapping of neutral dielectric particles and atoms have been demonstrated [2, 3]. They also demonstrated non-destructive manipulation of living cells such as bacteria later [4].

Chu and his colleague extended Ashkin's method to trap atoms laser cooling and trapping

of atoms to dimensions less than the optical wavelength [5]. He received the Nobel Prize in physics in 1997 along with Claude Cohen-Tannoudji and William Daniel Phillips by this work. Indeed it was a very big breakthrough to control atom in the 1 \AA scale.

Until now, this technique has been widely applied to physics and biological studies. Usually laser trapping is applied to manipulate single micrometer to nanometer-sized particles, and now being developed to combine with single molecule spectroscopy [6].

1.1.2 Principle of laser trapping

Laser trapping is a physical phenomenon which is described by the interaction between light and objects. Traditionally, optical force enables to trap and manipulate small particle is clarified into two parts: gradient force and scattering force. The former is directed along the spatial laser gradient and the latter is along the direction of light propagation. For stable trapping of objects, three-dimensional intense gradient force is necessary. This condition is provided when very sharp light intensity change is achieved by using an objective lens with high numerical aperture (N.A.). The steep gradient force which transfers the object to the focal region must be larger to exceed the scattering force which moves the object away from the focal region.

In developing a theoretical treatment of optical trapping, there are two limiting cases for which the force on a sphere can be readily calculated. When the trapped sphere is much

larger than the wavelength of the trapping laser, the conditions for Mie scattering are satisfied [7]. Refraction of the incident light by the sphere corresponds to a change in the momentum carried by the light. By Newton's third law, changed momentum of photon and that of the object should be equal. The force on the sphere, given by the rate of momentum change, is proportional to the light intensity (Fig. 1.1). When the refractive index of refraction of the particle is greater than that of the surrounding medium, the optical force arising from refraction is in the direction of the intensity gradient (Fig. 1.2a) [8]. Conversely, for an index lower than that of the medium, the force is in the opposite direction of the intensity gradient (Fig. 1.2b).

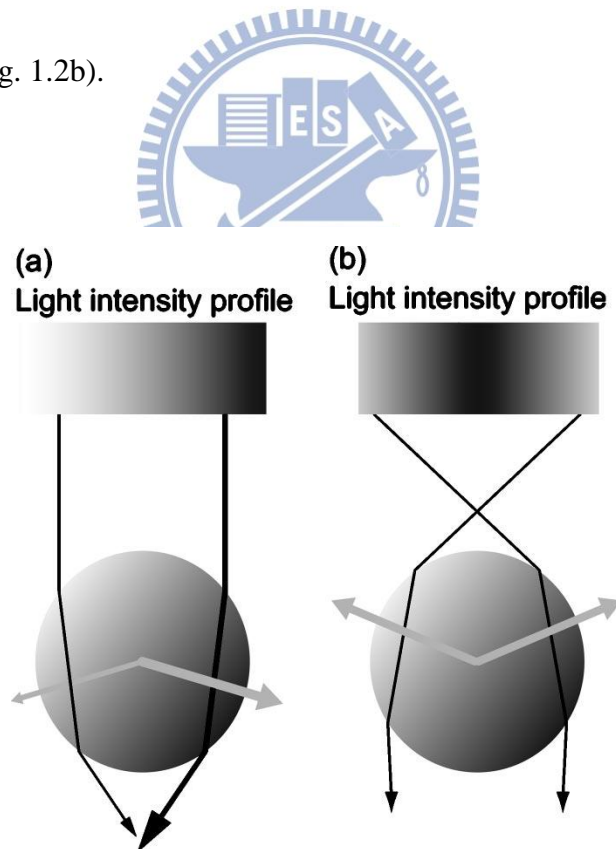


Fig. 1.1 Ray diagram shows difference of the direction of gradient force (gray arrows) induced by unfocused (a) and focused (b) light.

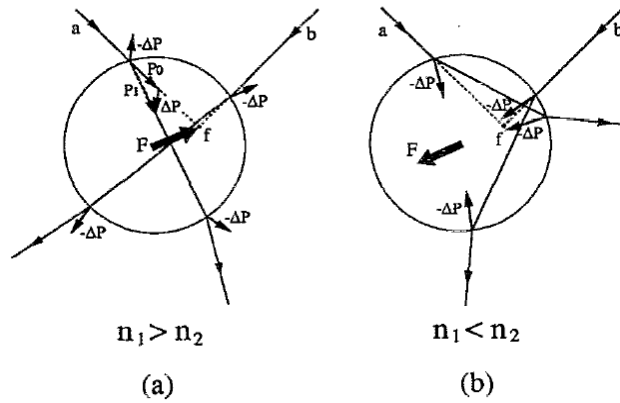


Fig. 1.2 Schematic drawing of the relationship between refractive indices of particle (n_1) and medium (n_2) and the direction of gradient force (F).

For another case, Rayleigh scattering are satisfied when the trapped sphere is much smaller than the wavelength of the trapping laser. The particle can be treated as a point dipole under this condition. We need to consider the interaction between an electric field of the light and dipole moment of the particle. Gradient and scattering forces are expressed in equation 1.1 and 1.2, respectively, where E and B denote electric field, and magnetic field. σ_p is the scattering cross section of a particle. c denotes the speed of light in vacuum. α in equation 1.3 is the polarizability of a particle under the light condition, where r is the radius of the particle, and ϵ_m is the dielectric constant of the surrounding medium. n_p and n_m are the refractive indices of the particle and the surrounding medium, respectively.

$$F_{grad} = \frac{1}{2} \alpha \nabla |E|^2 \dots \dots \dots (1.1)$$

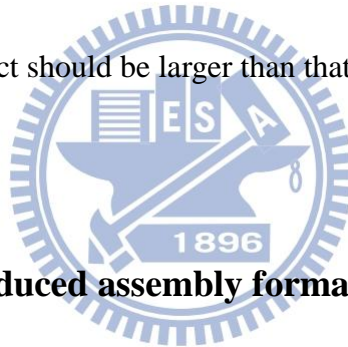
$$F_{scat} = \frac{n_m \sigma_p}{c} \langle E \times B \rangle_t \dots \dots \dots (1.2)$$

$$\alpha = 4\pi \epsilon_m r^3 \frac{\left(\frac{n_p}{n_m}\right)^2 - 1}{\left(\frac{n_p}{n_m}\right)^2 + 2} \dots \dots \dots (1.3)$$

As the high N.A. objective lens is employed, the trapping potential becomes to the equation 1.4. When trapping potential energy overcomes the energy of a Brownian motion $k_B T$, where k_B is the Boltzmann constant and T is the temperature in Kelvin, photon pressure makes it possible to control the object.

$$U = -\frac{1}{2}\alpha|E|^2 \dots\dots\dots (1.4)$$

Similarly, as in Ray optics, the condition for driving the object toward the focal region, the refractive index of the object should be larger than that of medium ($n_p > n_m$)



1.1.3 Laser trapping-induced assembly formation

Extending the laser trapping technique allowed scientists to investigate the interaction of particles, such as colloids [9], polymers and membranes [10]. Laser trapping technique has been demonstrated to assemble small particles of colloids and polymers [11, 12] to create their assembly which is larger than the focal spot size. Masuhara and his colleagues investigated the assembly formation of many polymer molecules under photon pressure [13-15] and its solvent dependence [16]. Fig. 1.3 describe schematic representation of assembly formation of Poly(N-isoprpyrl acrylamide) (PNIPAM) that induced by focusing of trapping light source into its solution [12].

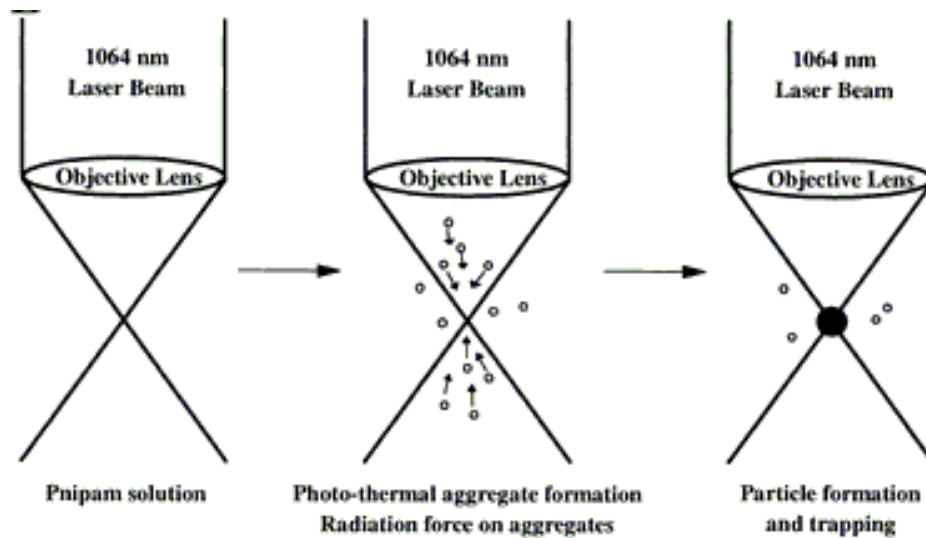


Fig. 1.3 Schematic view of PNIPAM assembly via photon pressure and phase transition [12].



On the other hand, heat generation by absorption of focused light is inevitable in laser trapping since both solvent and solute can absorb the trapping laser light. It induces Marangoni convection flow [17, 18] and enhances mass transfer that increases molecular transportation which should cooperate with photon pressure to collect molecules in liquid-liquid system [19]. Recently Uwada *et al.* visualized the convection flow under laser trapping by using gold nanoparticle as probe of the motion of the particle in the solution with Rayleigh scattering microscopy as shown in Fig. 1.4. [20].

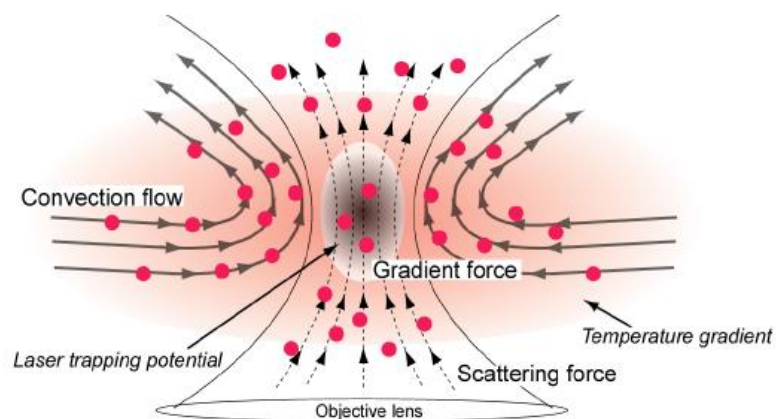


Fig. 1.4 Schematic picture of proposed transportation of nanoparticles due to the convection flow under the laser trapping in water. [20].

Previously reported molecular assembly formations, such as PNIPAM assembling, induced by laser trapping imply a possibility of the formation of more advanced molecular assembling not only collect the solutes but also the crystallization. Tsuboi *et al.* reported the assembling of several amino acids under laser trapping in solution by using Raman scattering and backward scattering detection [21]. They concluded that laser trapping induced assembly is formed by trapping clusters of solute molecules. They also examined laser trapping of Lysozyme and observed small assembly formation during trapping laser irradiation. They can observe the crystal of lysozyme only after a few days later of trapping laser irradiation [22]. It suggests crystallization could be initiated from a protein aggregate which formed by photon pressure during trapping. We can find other laser trapping crystallization study of Lysozyme from Rubinsztein-Dunlop's group. They applied trapping to induce the crystal growth [23] and investigated directional crystal growth under trapping

[24, 25]. However no *in-situ* and real-time laser trapping crystallization of protein has been done yet.

1.1.4 Laser trapping by applying pulse laser

As we mentioned above, conventional laser trapping technology typically use CW laser as a light sources of trapping that need only a few mW power to investigate tweezing of micrometer objects in three dimensions. While CW tweezers have been tremendously successful, femtosecond pulse lasers provide extremely high pulse peak energy that allow to access nonlinear processes within trapped particles, such as multi-photon absorption and harmonic generation.

Malmqvist and co-workers have demonstrated second harmonic generation from optically trapped nonlinear Rayleigh particles using a femtosecond titanium-sapphire laser [26]. Xing and co-workers have presented numerical modeling and theoretical analysis which predicts that femtosecond laser trapping are entirely feasible [27].

Dholakia and his colleagues investigated the relative Q-values in the femtosecond and CW regimes shows that femtosecond laser trapping are just as effective as CW laser trapping [28]. This verifies that an average power is playing key role rather than the peak power for optical trapping. They also demonstrate simultaneous laser trapping and *in-situ* control of two-photon fluorescence (at 400 nm) from dye-doped polymer microspheres with

femtosecond laser. A distinctive advantage in using femtosecond tweezers rather than CW tweezers is that the characteristically high peak powers of femtosecond pulses can be used to exploit nonlinear optical processes.

Tamai and colleagues investigated nanometer-sized CdTe quantum dots (QDs) in D₂O can be optically trapped by a high repetition-rate picosecond Nd: YLF laser with an input power as low as 100 mW [29], while an extreme high power (20 W) is necessary in CW laser trapping. A large two-photon absorption (TPA) cross section of 10⁴–10⁵ GM for CdTe QDs makes it possible to detect the trapping process with TPA induced luminescence.

Recently, Okamoto's group demonstrated a novel phenomenon of trapping arising from nonlinear polarization when we trap gold nanoparticles (AuNPs) by femtosecond near-infrared (NIR) laser pulses [30]. The stable trap site of AuNPs is split into two equivalent positions. The trap positions are aligned along the direction of the incident laser polarization. The results were successfully interpreted in terms of the nonlinear polarization caused by the femtosecond pulses.

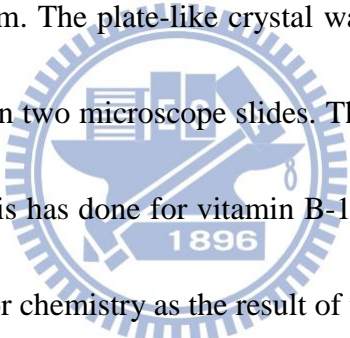
1.2 Crystallization

In this dissertation, I demonstrate new crystallization method induced by femtosecond pulse laser trapping. Crystallization is closely related to our daily life such as the salt isolation from seawater and diamond formation in the deep earth under high temperature

and pressure. Crystal provides molecule packing information and is used in wide fields of science and technology.

1.2.1 History of biomolecular crystallization

The history of macromolecular crystallization described by McPherson can be traced back to more than 150 years ago [31]. The first published observation of the protein crystallization was reported by Hunefeld in 1840 [32]. They reported the crystallization of hemoglobin from the earthworm. The plate-like crystal was observed when the blood of an earthworm was pressed between two microscope slides. The first structural determination of biomolecule with X-ray analysis has done for vitamin B-12 in 1957 by D. C. Hodgkin [33]. She received the Nobel prize for chemistry as the result of this research.



Crystallization has been studied for long time, however, its process is very complex and crystallization of biomolecule is still very difficult. In order to understand the fundamentals of crystallization to obtain better crystals, massive efforts were made on optimized crystallization and crystal growth of basic molecules, such as small organic compounds and amino acids. Crystallization of amino acids, which are the basis unit of protein, is important works for protein crystallization. We have been conducting laser trapping crystallization study and already possess knowledge for the crystallization of amino acids, especially on glycine. Therefore we employed amino acid, glycine, in this work. Until now, crystallization

of protein is still quite empirical. By studying the crystallization of amino acids, we are also expecting to gain further understanding of crystallization of proteins from the results of this study.

1.2.2 Crystallization theory

Crystallization is a phase separation process and used as a purification method. Usually, concentration of solution for crystallization must be at supersaturation which is achieved by many variable methods such as vapor pressure, temperature and pH valve. The crystallization process consists of two major parts; nucleation and crystal growth. The birth of a new crystal is called nucleation. It indicates that molecular aggregate becomes larger than the critical size. Traditionally, the classical nucleation theory has been employed for the nucleation process, but it starts with tiny size and is difficult to observe experimentally [34]. After nucleation, a subsequent process is known as crystal growth where nuclei grow larger. Molecules are continuously packing with each other in the regular ordering (Fig. 1.5).

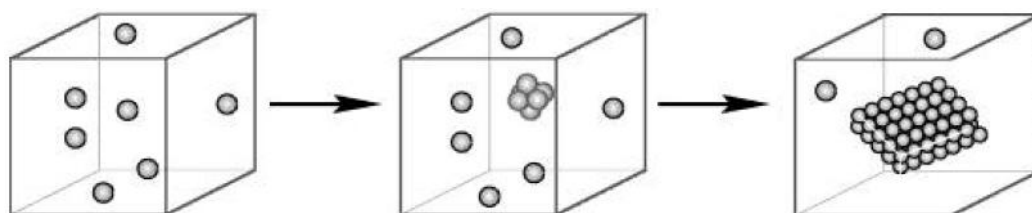


Fig. 1.5 Schematic drawing of classical nucleation theory, crystal growth by packing of molecules [34].

However, a number of differences between theoretical predictions and experimental results suggest that nucleation of solids from solution does not proceed via the classical nucleation theory but follows more complex routes. In this account, the development of the modern two-step model was discussed. In the two-step model, a highly disordered dense liquid droplet was formed, after that the cluster inside the droplet reorganized into an ordered alignment [35, 36].

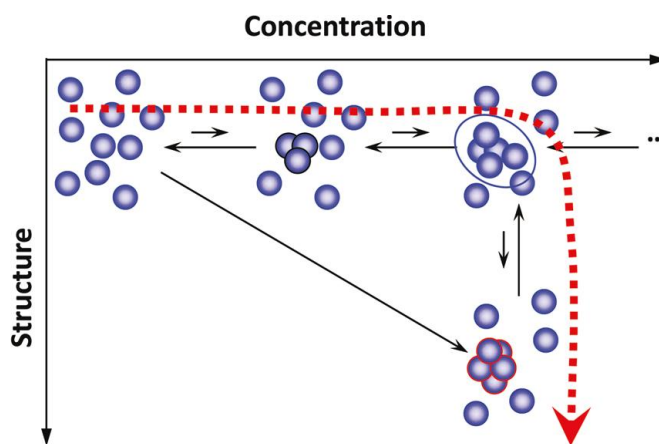


Fig. 1.6 Schematic illustration of the two-step mechanism of nucleation of crystals (dot line) [35].

The experiments discussed below demonstrate that nucleation of crystals of the protein lysozyme proceeds in two steps: the formation of a droplet of a dense liquid, followed by nucleating a periodic crystal within the droplet. When the dense liquid is not stable but has a higher free energy than the dilute solution ($\Delta G^0 > 0$, represented by the upper curve in Fig. 1.7, the dense phase is metastable with respect to both the solution and the crystals and only

exists as a density fluctuation of a limited lifetime; If the dense liquid is stable with respect to the dilute solution ($\Delta G^0 < 0$, represented by the lower curve in Fig. 1.7), the nucleation of crystals occurs inside macroscopic droplets of this phase.

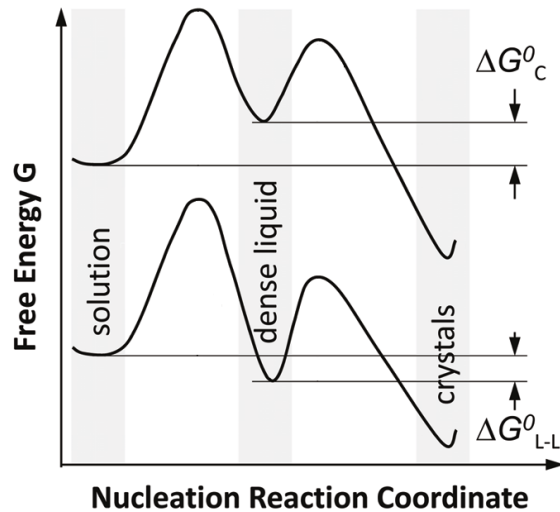


Fig. 1.7 Free energy diagram for possible crystallization processes [34].

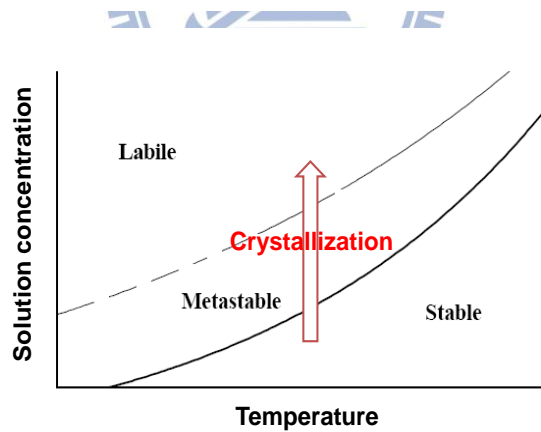


Fig. 1.8 Phase diagram showing the solubility depends on temperature and concentration. Once solution became highly saturated with higher free energy in the labile or metastable region, nucleation could take place, causing a reduction of free energy and the phase returned to the stable region.

1.3 Light-induced crystallization methods

Light-induced crystallization can be realized with various light sources through different mechanisms, such as photochemical and nonphotochemical processes where applicable light sources are Xe lamp, CW laser or pulse laser at different wavelengths ranging from UV to NIR region.

1.3.1 Kerr effect crystallization

In 1996, Garetz *et al.* discovered that intense nanosecond NIR laser pulses (pulse duration: 20 ns, repetition rate: 10 Hz, wavelength: 1.06 μm) can induce nucleation of urea solution. The solutions are transparent at the incident wavelength, a photochemical mechanism is unlikely. This phenomenon was named as nonphotochemical laser-induced nucleation (NPLIN). The needle-shaped crystals that initially form tend to be aligned parallel to the electric field vector of the light. They suggested that the electric field-induced realignment of urea molecules results in cluster formation, and this mechanism is known as the optical Kerr effect [37]. Nucleation of glycine was also demonstrated and the polymorph of glycine was controlled by changing polarization of laser beam [38, 39] or by additionally applying strong DC electric field to enhance the optical Kerr effect [40].

1.3.2 Photochemical reaction-induced crystallization

Okutsu *et al.* have reported photochemical reaction-induced crystal growth and morphology control of anthracene [41]. Furthermore, they have investigated photochemical reaction-induced nucleation of hen egg-white lysozyme (HEWL) [42], thaumatin [43], and ribonuclease A (RNaseA) [44]. In the lysozyme crystallization experiment, they exposed UV light (wavelength: 280, 300 and 400 nm) from Xe lamp (wavelength: 200-800 nm, USHIO UXL-300D) to supersaturated but metastable lysozyme solution and produced photochemical intermediate (Fig. 1.9). The photochemical product, the protein dimer, behaved as the smallest cluster of nucleation. Okutsu gave a representative demonstration of photochemical reaction-induced nucleation. However, it is not known for sure how radical formation affects the purity of the obtained protein crystal.

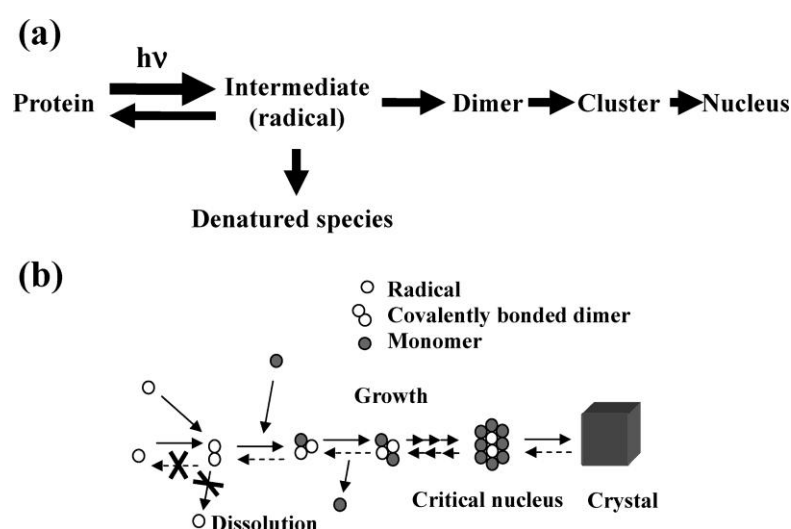


Fig. 1.9 Mechanism of (a) the photochemically induced nucleation of lysozyme, and (b) enhancement of protein crystallization by a photochemical reaction [44].

1.3.3 Amplified femtosecond laser-induced crystallization

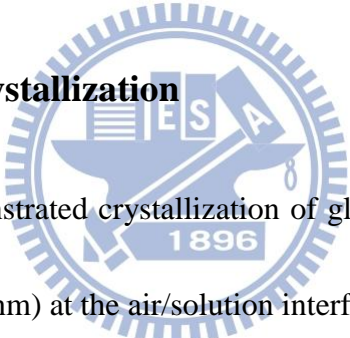
Hosokawa et al. was firstly demonstrated HEWL crystallization by amplified femtosecond laser in 2003 [45]. Besides, urea [46], anthracene [47] and 4-(dimethylamino)-N-methyl-4-stilbazolium tosylate (DAST) [48] crystallizations were also reported in following years. Femtosecond laser-induced crystallization is triggering nucleation by multiphoton absorption of solvent leading to optical breakdown and is less related with solute. When an intense femtosecond laser light is focused into water, multiphoton absorption of water induces nonlinear phenomena such as shockwaves and cavitation bubbles. These nonlinear phenomena were also described as laser tsunami.

Our collaborator Uwada also demonstrated the amplified fs laser induced crystallization of glycine and lysozyme from its supersaturated solution [49]. Pulse energy and repetition rate dependences show that the frequency of cavitation bubble generation induced by multiphoton absorption of water is playing a key role for nucleation process. The local concentration change around the cavitation bubble will probably induce nucleation of crystals. They also observed significant increase of crystallization probability by focusing fs pulses at the air/solution interface. They ascribe the reason of observed increasing of crystallization probability to molecular adsorption at the interface where restricted freedom of molecular motion may improve molecular ordering at the generated bubble surface.

Recently, high-speed and high-resolution photography have also been used to investigate

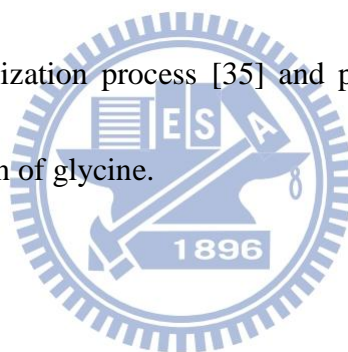
laser-induced cavitation bubble behavior and the subsequent nucleation of crystals. The bubble size was expanding and shrinking. In order to discuss the importance of Rayleigh bubble to crystallization, Murai *et al.* increased the viscosity of lysozyme solution by adding agarose gel against protein diffusion from the focal point and recorded the conformation change of bubbles [50]. They successfully observed the formation of locally high concentration region induced by bubble conformation change led to elevate crystallization probability around the surface of bubble.

1.3.4 Laser trapping crystallization



Sugiyama *et al.* have demonstrated crystallization of glycine by focusing a near-infrared laser beam (wavelength: 1064 nm) at the air/solution interface. It was the first observation of the crystallization only by focused irradiation. They named this method as “laser trapping crystallization”. The initial crystallization was observed by a CCD camera that the glycine crystal grew from focus to a certain size within a few seconds [51]. They also observed that crystal growth of glycine was accelerated by focusing a CW 1064-nm laser beam at a position. The crystal growth rate depended on where the focused laser placed against crystallographic axes [52]. They also reported that crystallization can be achieved in unsaturated glycine solution with this crystallization method [53]. They have investigated the method to control crystal polymorph by tuning laser power. It was found that the

competing result between photon pressure and temperature elevation at a certain high laser power led to the probability increase to find γ -polymorph glycine crystal, which is not available under ambient conditions [54]. Yuyama *et al.* have demonstrated the formation of a millimeter-scale dense liquid droplet of glycine induced by laser trapping effect [55]. The droplet would form after focusing a CW NIR laser beam at the glass/solution interface of a thin film of its supersaturated heavy water solution. Once the droplet formed, they found that crystallization starts immediately just after the focal position is shifted to the air/solution interface. It is considered that the dense droplet formation is possibly the early stage of the multistep crystallization process [35] and plays an important role in photon pressure-induced crystallization of glycine.

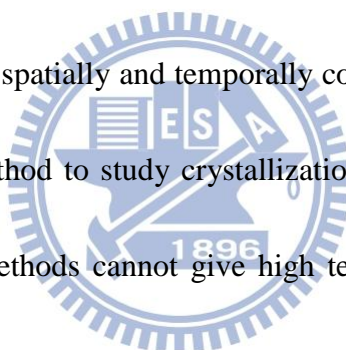


1.4 Motivation

Our purpose of this work is to explore a new laser trapping crystallization method. In this study, we applied femtosecond laser pulses on laser trapping crystallization of glycine. Earlier studies related to the laser trapping by femtosecond pulse imply that femtosecond laser can be utilized as an efficient trapping light source for the crystallization [30]. Therefore we can expect that application of femtosecond laser can bring a new and better optical crystallization methodology.

High peak intensity of amplified femtosecond laser usually leads nonlinear multiphoton process and ablation of the water or solvent. To prevent bubble-induced crystallization, we kept the laser energy sufficiently low to prevent the generation of cavitation bubble. Another possibility of the ablation under femtosecond laser pulse trapping, namely an ablation of generated crystal, will be taking into account. We also demonstrate new single crystal formation method by combining fs pulse and CW lasers.

Higher efficiency of laser trapping with fs pulses can be expected to give better temporal controllability. Thus, through single crystal formation method by a combination of fs and CW laser, we can demonstrate spatially and temporally controlled crystallization of glycine. It will be a very powerful method to study crystallization dynamics and mechanism since conventional crystallization methods cannot give high temporal and spatial controllability that we will achieve only fs/CW combined laser trapping crystallization method.



2. Experiment

2.1 Materials

Glycine (99.0%, Wako Pure Chemical) in the form of white powder was used without further purification. D₂O (>99%, Sigma-Aldrich) as a solvent was filtrated with a syringe filter (pore size; 0.22 μm, SLGV 013 SL, Millipore) before dissolving glycine. Concentration of glycine/D₂O solution is 2.40, 2.64, and 3.43 M which supersaturation values are 0.9, 1.0, and 1.32, respectively. Solute molecules in the solution were ensured to be totally dissolved by heating with a water bath to 60°C for 24 h and then decreased the temperature of the solution stepwise until it returned to room temperature (~25°C). Prior to the laser trapping crystallization experiments, solutions were aged for 1 to 7 days to ensure the absence of spontaneous crystallization. Here we used deuterated water as solvents to suppress temperature elevation due to 1064 nm trapping laser absorption.

A home-made closed glass container which was made by gluing (Shin-Etsu Silicone, 1 component RTV) a cut glass vial (Nichiden-Rika glass) on a cover glass (18 × 18 mm) was used as experimental container (fig 2.1(a)). The glass container was sunk in detergent at least for one day, and then washed by purified water repeatedly and cleaned by plasma cleaner before using. After wet and dry cleanings surface of all glass containers became highly hydrophilic. Applied solution to clean and hydrophilic surface spreads and covers

whole glass surface stably. A portion of glycine solution (15 μL) was poured into a glass container. The D_2O of glycine solution can easily spread on the bottom of the glass container and formed a thin solution layer without touching the glass wall as shown in Fig. 2.2a. The shape of the D_2O of glycine solution is convex. The initial solution layer thickness was about 120 μm .

For volume dependence experiment in chapter 3, another home-made glass container (Fig. 2.1(b)) which was made by gluing short glass tube and cover glass ($24 \times 30 \text{ mm}$) was used. Different solution volume can be applied in this container. Before usage of the containers, containers were washed with detergent, acetone and purified water repeatedly. Washed containers were further cleaned by nitrogen plasma treatment (10 minutes with nitrogen gas flow rate of 40 cc/min). After wet and dry cleanings surface of all glass containers became highly hydrophilic. As well as in the other container, glycine solution can easily spread on the bottom of the glass container and formed a concave solution layer with touched the glass wall (Fig. 2.2b). The initial solution layer thickness was about 75, 200, 350, 500 μm with 150, 175, 200, 225 μL solution volume, respectively.

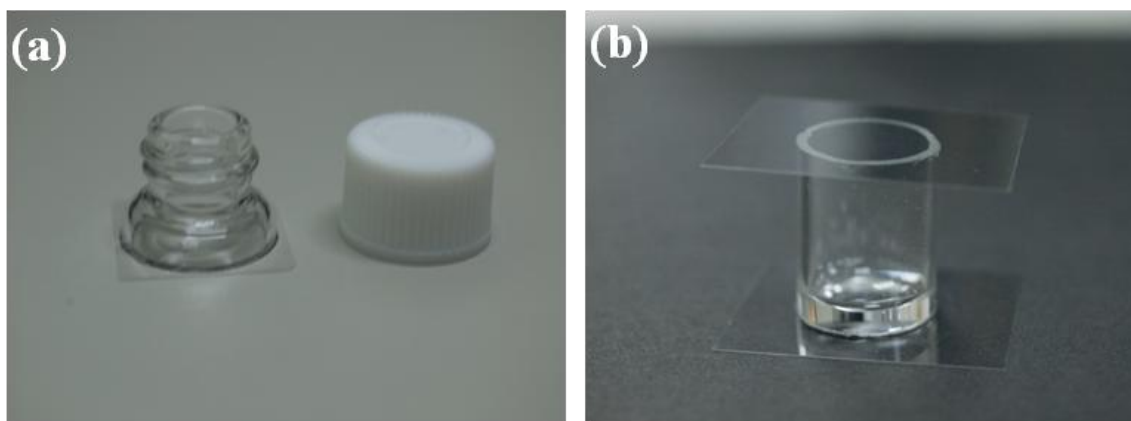


Fig. 2.1 Pictures of container made of (a) cut glass vial and (b) short glass tube.

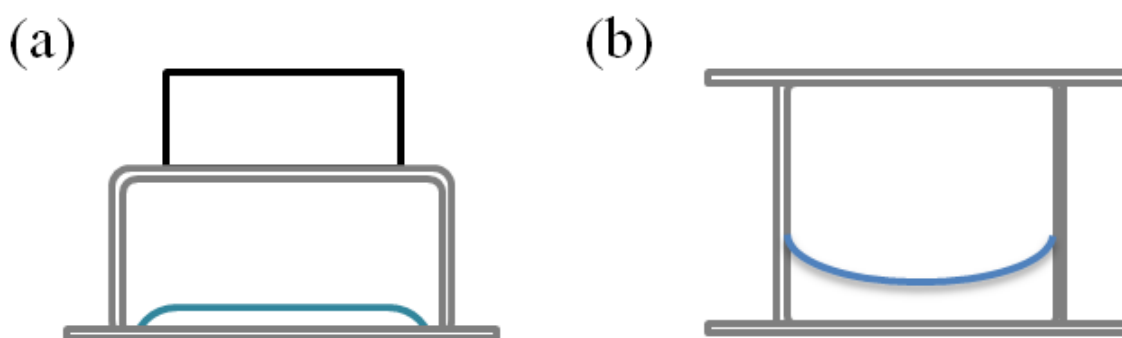


Fig. 2.2 Schematic drawing of surface shape: (a) cut glass vial and (b) short glass tube.

2.2 Property of glycine

Protein is a biological macromolecule composed of 20 common amino acids. Glycine ($\text{NH}_2\text{CH}_2\text{COOH}$) is the simplest amino acid with lowest molecular weight and a colorless, sweet-tasting crystalline solid (Fig. 2.3). It has been frequently studied in the field of crystallography.

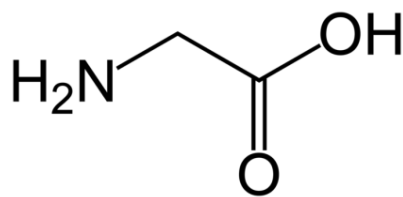


Fig. 2.3 The chemical structure of glycine.

From small angle X-ray scattering (SAXS) study of glycine supersaturated aqueous solution, it is suggested that zwitterionic form glycine molecules exist as dimers in supersaturated solution [56]. In the supersaturated solution, dimers and water molecules aggregated with each other due to Columbic interactions and hydrogen bonding, form liquid-like cluster. The solubility of glycine in aqueous solutions was determined by means of evaporating and weighing the residue [57]. Table 2.1 shows the solubility of glycine in water and deuterated water. At 20°C, the molar concentration of saturated glycine/D₂O solution is 2.4 M. Solubility of glycine solution with using H₂O or D₂O as the solvent do not show obvious difference.

Table 2.1 Solubility of glycine in H₂O and D₂O [2].

| Temperature (°C) | Glycine weight (g) to 100 g of the solvent | |
|------------------|--|------------------|
| | H ₂ O | D ₂ O |
| 20 | 21.85 | 21.76 |
| 30 | 26.45 | 26.90 |

Glycine crystal shows three polymorphs: α , β and γ . The α - and β -forms crystal in the monoclinic system with centrosymmetric space groups P2₁/n and P2₁, respectively. γ -form crystallizes in the trigonal-hexagonal system with non-centrosymmetric space group P3₂

[58-61]. The shape difference between α - and γ -polymorph glycine crystals can be clearly distinguished in Fig. 2.4.

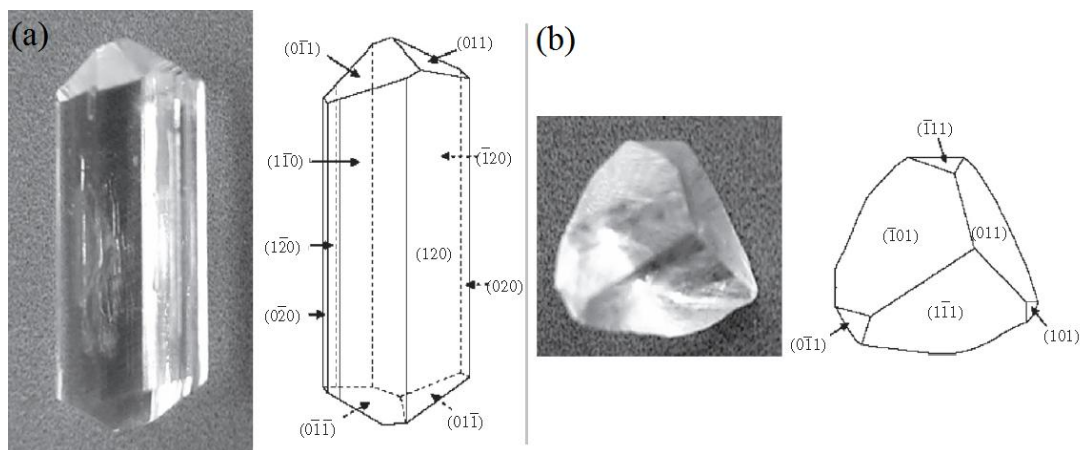


Fig. 2.4 Schematic diagram of the morphology of the (a) α - and (b) γ -glycine single crystals [4].



Usually, commercially available glycine powder contains mixture of α - and γ - polymorph. β -polymorph is unstable and difficult to exist for a long time, and easily transform to α -form. γ -polymorph crystal is the most thermodynamically stable among these three polymorphs. But spontaneous crystallization almost gives kinetically stable α -polymorph under moderate experimental condition. Crystal of γ -polymorph is preferentially obtained under relatively hard conditions for crystallization such as using acid, base or using heavy water solution [62]. Comparing to traditional crystallization method, it is difficult to prepare γ -polymorph crystal just under using heavy water as solvent in laser trapping crystallization. The success

of crystallizing γ -polymorph seems to depend on optical parameters (i.e., power and polarization of laser) in laser trapping crystallization method [54, 63] less determined by the solvent. Ethanol should be used to precipitate β -polymorph from a saturated water solution, however a mixture of the α - and the β -polymorphs are always obtained [59, 61].

The transformations among these three polymorphs are very complicated [59]. Although α -polymorph is quite stable at room temperature, it transforms to γ -polymorph after several months. The transformation rate is highly dependent on the humidity of environment and higher the humidity transformation rate accelerated. β -polymorph refers to transform to α - but not γ -polymorph under high humidity, but it can be preserved well in dried environment. β -polymorph also transforms to α -polymorph with heating below 100°C or mechanical shocks such as crush. γ -polymorph is quite stable at room temperature but it transforms to α -polymorph at 165°C. Reverse transformation does not take place immediately even after γ -polymorph is cooled down to room temperature [60].

Glycine is frequently employed in crystallization study. Usage of this well-known simple amino acid will enables to focus studying to understand the mechanism of femtosecond laser-induced crystallization itself.

2.3 Laser mode

A laser can be classified as continuous wave (CW) or pulse depending on whether the

power output is essentially continuous over time or its output takes the form of pulses of light. CW operation of a laser means that the laser is continuously pumped and continuously emits light with constant frequency. Pulsed operation of a laser means that the emitted light in the form of optical pulses with changeable amplitude.

2.3.1 Continuous wave laser light source

Nd:YVO₄ is one of the most efficient laser host crystal currently existing for diode laser-pumped solid-state lasers. Its large stimulated emission cross-section at lasing wavelength, high and wide absorption coefficient and bandwidth at pump wavelength, high laser induced damage threshold as well as good physical, optical and mechanical properties make Nd:YVO₄ an excellent crystal for stable, high power and cost-effective diode pumped solid-state lasers. Recent developments have shown that Nd:YVO₄ can produce powerful and stable IR, green, blue lasers with the design of Nd:YVO₄ and frequency doubling/tripling crystals. A Nd:YVO₄ laser (wavelength: 1064 nm, J20-BL10-106Q, Spectra Physics, Fig. 2.5) was used as the continuous wave light source in this study. A NIR laser light output from laser head (BL10) was controlled by a computer which was connected to the power supply (J20). The output power of the laser is determined by the current to the laser diode.

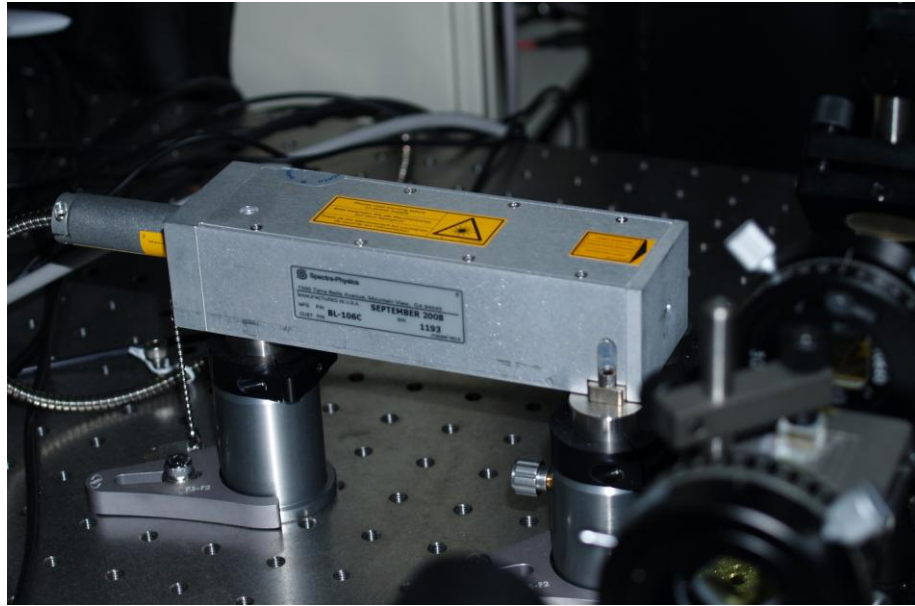


Fig. 2.5 Picture of Nd:YVO₄ laser, J20-BL10-106Q, used in this study.

2.3.2 Femtosecond laser light source

Femtosecond (fs) pulse train generated by a mode-locked Ti:Sapphire laser (wavelength: 700-900 nm, repetition rate: 80 MHz, pulse duration: 150 fs, Tsunami, Spectra Physics, shown in Fig 2.6a) which is pumped by a CW solid-state green laser (wavelength: 532 nm, Millennia Pro, Spectra Physics, shown in fig 2.6b) at about 8 W, was used as fs pulse laser for trapping. A prism sequence and a slit were used for dispersion control and wavelength selection, respectively. A full width at half maximum (FWHM) of the spectrum and central wavelength of the laser light were determined to about 12 nm and 800 nm by a fiber optic spectrometer (USB4000, Ocean Optics).

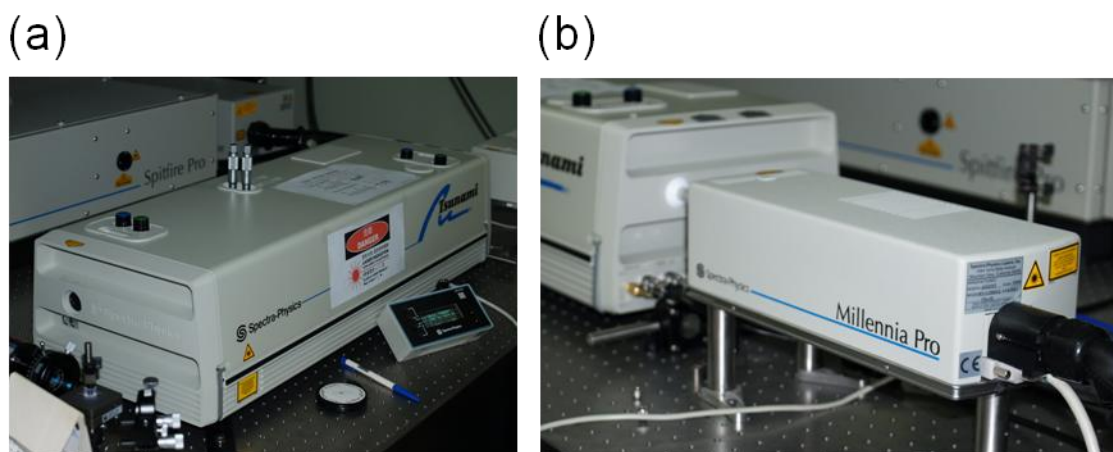


Fig. 2.6 Picture of (a) mode-locked Ti:sapphire laser, Tsunami and (b) pump laser, MillenniaPro.

2.4 Microscope setup for imaging of crystallization behavior

Figure 2.7 shows a schematic drawing of optical setup for laser-induced crystallization experiment. Microscope setup is based on an inverted microscope (Olympus, IX71). Temperature and humidity were controlled to be around 23~25°C and 50~60% by air conditioner, respectively. We use two different laser light source for trapping experiment. One is NIR Ti:Sapphire laser at 800 nm, which can operate both in femtosecond pulse and continuous wave. Another is NIR CW 1064 nm Nd:YVO₄ laser (J20-BL10-106Q, Spectra Physics). Both lasers were introduced into the microscope and focused to the air/solution interface of sample solution through a 60× objective lens (N.A. 0.90). In order to achieve optimal trapping condition, laser beam was expanded and collimated to fully use a back

pupil diameter of microscope objective lens (~8 mm). A 633 nm CW He-Ne laser (LASOS, LGK 7628, ~5 mW) was also introduced into the microscope coaxially with two NIR lasers for checking solution surface height and focus height of NIR laser.

Crystallization behavior around the laser spot was monitored by bright field transmission imaging method by using a halogen lamp as an illumination light source and recorded by CCD camera. Sample solutions were covered to suppress spontaneous evaporation of solution during the laser irradiation.

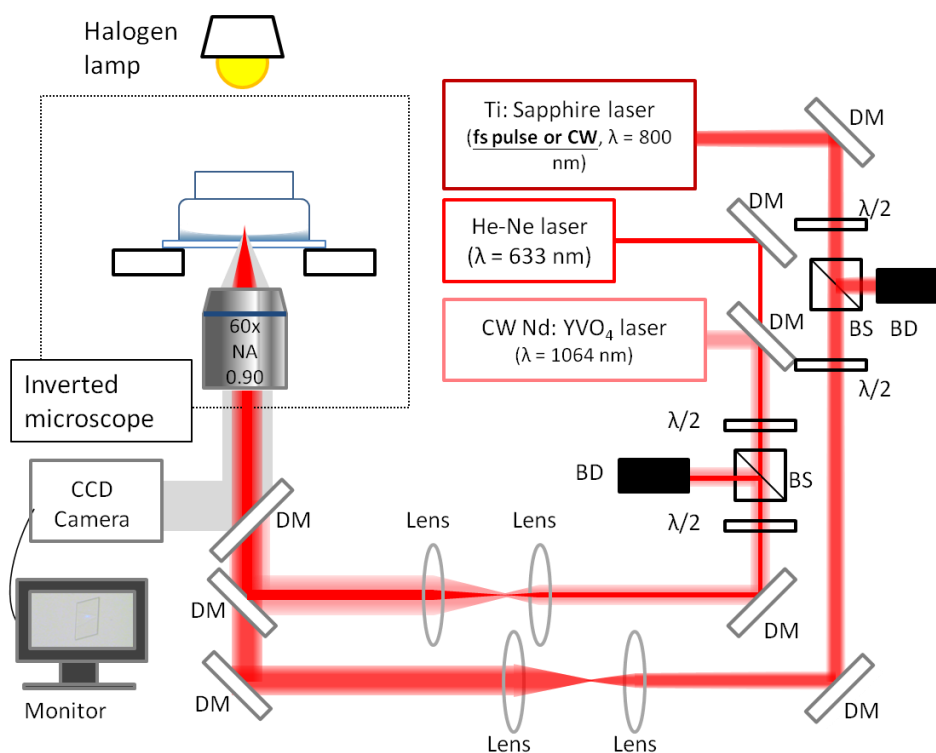


Fig. 2.7 Optical set up of laser-induced crystallization system.

2.5 Fourier transfer infrared spectra measurement

Fourier transform infrared spectroscopy (FTIR) is a technique which is used to obtain an

infrared spectrum of absorption and emission of a solid, liquid or gas. An FTIR spectrometer simultaneously collects spectral data in a wide spectral range. This wide spectral measurement is a significant advantage compared to a dispersive spectrometer which measures intensity over a narrow range of wavelengths at a time. After the measurement, computer will process Fourier transform algorithm is used to turn the raw resultant data into the desired spectral data, namely light absorption data for each wavelength.

In this study, Attenuated Total Reflectance-Fourier transform infrared (ATR-FTIR) spectroscopy was used to obtain detailed information of the polymorph of glycine crystal.

ATR is a sampling technique used in conjunction with infrared spectroscopy which enables samples to be examined directly in the solid or liquid state without further preparation.

Figure 2.8 is describing a principle of multiple reflection ATR system. An infrared beam is directed onto an optically dense crystal with a high refractive index at a certain angle through an optical waveguide. In the case of a glycine crystal, it is crushed and pressed to ATR crystal for attaining direct contact. This internal reflectance creates an evanescent wave that extends beyond the surface of the crystal into the sample. The penetration depth into the sample is typically between 0.5 and 2.0 micrometers. Consequently, there must be good contact between the sample and the ATR crystal surface. The evanescent wave will be attenuated in regions of the infrared spectrum where the sample absorbs energy. Transmitted light is then collected by a detector and the system then generates an infrared spectrum.

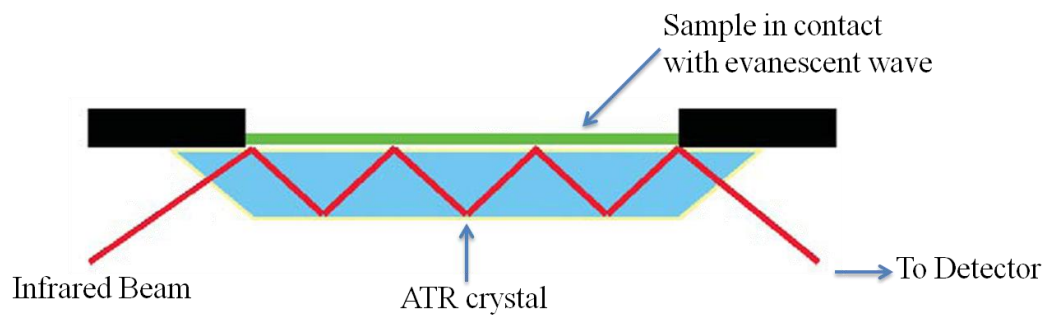


Fig. 2.8 A multiple reflection ATR system. Light undergoes multiple internal reflections in the ATR crystal of high refractive index, shown in yellow. The sample is in contact with the crystal.



3. Continuous Wave Laser-Induced Crystallization

To compare CW and fs laser-induced crystallization in the next section, we studied CW laser trapping crystallization under different experimental parameters as for the first step. Laser trapping crystallization with high power laser (0.8~1.4 W) was examined [54, 63], and we found crystallization of glycine was always successful under such high laser power condition. We also examined the crystallization efficiency at low power (0.2~0.6 W) laser trapping crystallization. We found power threshold of laser trapping crystallization on CW laser trapping. We had also checked solution volume dependence of laser trapping crystallization.



3.1 Power dependence of laser trapping crystallization

CW 1064 and 800 nm lasers were used. It should be necessary to check the efficiency of laser trapping crystallization from low to high power range. We define the crystallization probability as follow; experimental observation time is restricted to 30 min. If crystallization is observed within 30 min, then it is counted as successful crystallization. If crystallization is not observed within 30 min, it is counted as failed case.

Heat generation by focused trapping laser cannot be ignored since long time laser irradiation will make the solvent evaporated. Although we tried to reduce the evaporation of

solvent by using a closed chamber as a container, solution height still slowly decreased. In this condition, the edge of the solution will possibly be dried and generate the crystal. A 1~2 hour laser irradiation time is not a suitable for spatiotemporally controlled laser trapping crystallization experiment. To avoid such complication, we decide a maximum laser irradiation time to be 30 min.

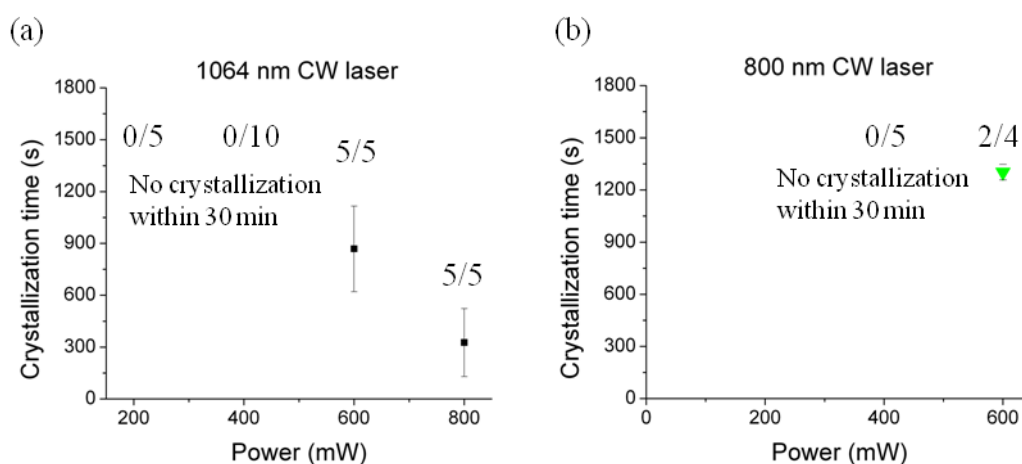


Fig. 3.1 Power dependence of laser trapping crystallization with a focused (a) CW 1064 nm and (b) CW 800 nm laser. Laser was focused to the air/solution interface of the glycine solution. Power of 200, 400, 600, and 800 mW CW laser was examined for 1064 nm with 1.0 SS solution; Power of 400 and 600 mW CW laser was examined for 800 nm with 0.9 SS solution. The examined crystallization time is 30 minutes.

We examined 1064 nm CW laser trapping crystallization with 200, 400, 600 and 800 mW trapping laser power and focusing to the air/solution interface of saturated solution (S.S. = 1.0) for 30 min. However we can observe crystal generation only with laser power above 600 mW as shown in Fig. 3.1a. CW laser trapping crystallization of 800 nm CW laser with 0.9 SS solution showed similar crystallization power dependency. We need more than 600

mW under examined condition as we can see in Fig. 3.1b. As we mentioned in previous section, crystallization can be initiated from high concentration region such as dense liquid droplet. Those results imply that the formation of local high concentration region generation by photon pressure is necessary for laser trapping crystallization, and 200 - 400 mW was not sufficient to induce nucleation of the crystal. Stronger power of laser will induce molecular assembly more efficiently [21]. It implies the local high concentration of solute induced by focused laser is depending on laser power. The growth rate of amino acid aggregates decreased with decreasing the laser power. We also can suggest that 30 min focusing of low power trapping laser is not enough strong to make surrounding of focal spot higher than the critical concentration for nucleation.

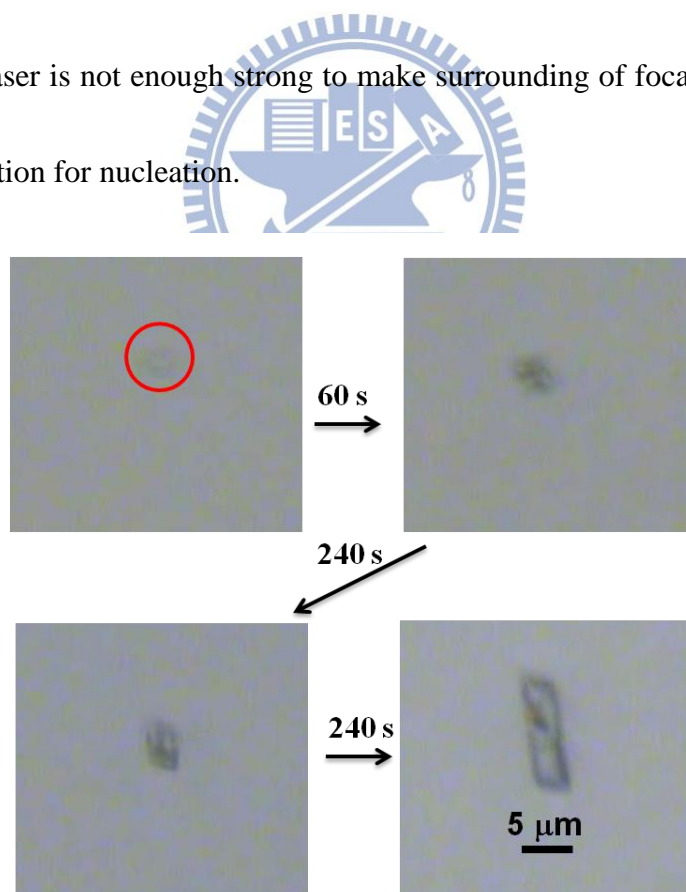


Fig. 3.2 Images of glycine crystal generation and growth by CW laser trapping. Saturation degree is 0.9 SS. Laser power is 600 mW.

Figure 3.2 shows snapshots of glycine crystal generation and growth at the air/solution interface. After few minutes of CW laser irradiation, the seed crystal was generated at the focal spot and trapped by the focused laser. The resulting crystal from low power laser showed the same crystallization process with the crystal from high power laser.

In spite of lower absorption coefficients of H₂O and D₂O at 1064 nm, heat effect by laser irradiation cannot be neglected when the intense laser beam is focused. The temperature elevation by laser irradiation has estimated by applying fluorescence correlation spectroscopy recently. Temperature elevation which is defined as $\Delta T/\Delta P$ (K/W in unit) at the focal spot is about 22-24 K/W in H₂O and 2 K/W in D₂O, respectively, with high NA objective lens (N.A. = 1.35) [64]. It suggests that if we use H₂O as a solvent, drastic temperature elevation increases the solubility of glycine and makes the crystallization more difficult. Therefore we have been using D₂O as a solvent of laser trapping crystallization in order to decrease the thermal effect [51]. We followed these information and used D₂O as a solvent of glycine solution to suppress temperature elevation during laser trapping.

When we use liquid thin film of glycine solution which was formed by dropping a small amount of solution onto the cover glass (solution layer thickness: <100 nm), it showed local surface deformation and height change during laser trapping crystallization process as shown in Fig. 3.3. Height was first lowered and liquid film become thin. After kept very thin condition of this liquid film for a while, surface height was started elevating and eventually

crystal formation was observed. The solution height elevation is attributed to the dense liquid droplet formation as reported [55]. In contrast to thin solution layer formed on cover glass, surface height/shape of the sample solution in cut glass vial showed no local surface deformation and negligibly slowly height decreasing. Figure 3.4 shows the solution height change during trapping laser focusing to the solution surface. A sample which was not irradiated showed typically less than a few μm decrease. Degree of height decreasing showed negligible power dependency in the range of 200~600 mW. All sample showed about 20 μm decrease for 30 min irradiation of trapping laser. Laser-induced surface deformation is almost negligible, and crystallization process may not be strongly affected.

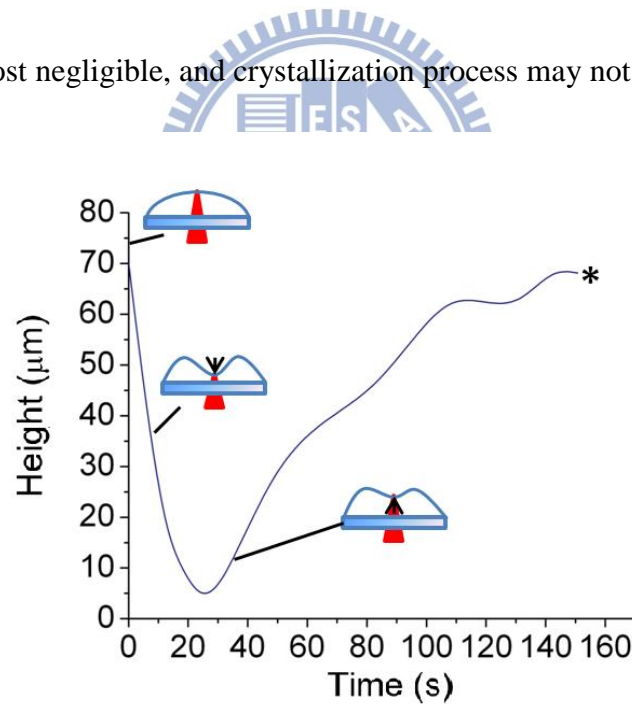


Fig. 3.3 Solution height change during 1064 nm CW laser irradiation in cover glass case, laser was focused to the air/solution interface of the thin glycine solution layer formed on the glass substrate. Above curve was obtained with 1.32 SS solution. Laser power is 1.0 W. Asterisk indicates the timing when crystallization occurred.

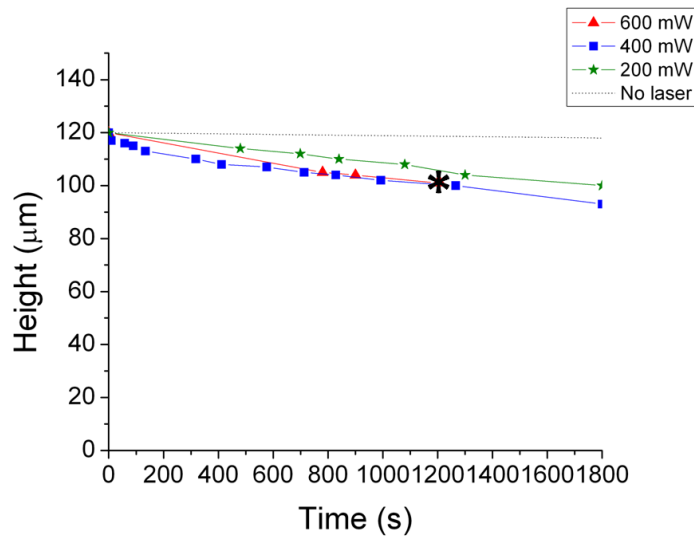


Fig. 3.4 Solution height change during 1064 nm CW laser irradiation in cut glass vial case. Laser was focused to the air/solution interface of the glycine solution. Above curve was obtained with 1.0 SS solution. 200, 400, 600 mW laser power was examined. Cut glass vial was used as a container. Asterisk indicates crystallization occurred in 600 mW case.



3.2 Volume/Thickness dependence of laser trapping crystallization

Previous studies of laser trapping crystallization suggest that spatial freedom and restriction of molecular transportation will have important effects. Here we have checked solution volume effect on laser trapping crystallization with a focused CW laser at the air/solution interface. Supersaturated solutions (ca. 3.43 M, S.S. = 1.32) and the short glass tube were used as a sample solution and container, respectively.

We found crystallization time depends on the volume as seen in Fig. 3.5. Interestingly, necessary time for crystallization increased linearly in time with increasing of solution volume/thickness. Figure 3.6 shows that solution thickness was not changed during laser

irradiation to the air/solution interface. The local surface height change and deformation were suppressed with a sealed glass tube. Although no surface deformation observed, crystal formation was confirmed.

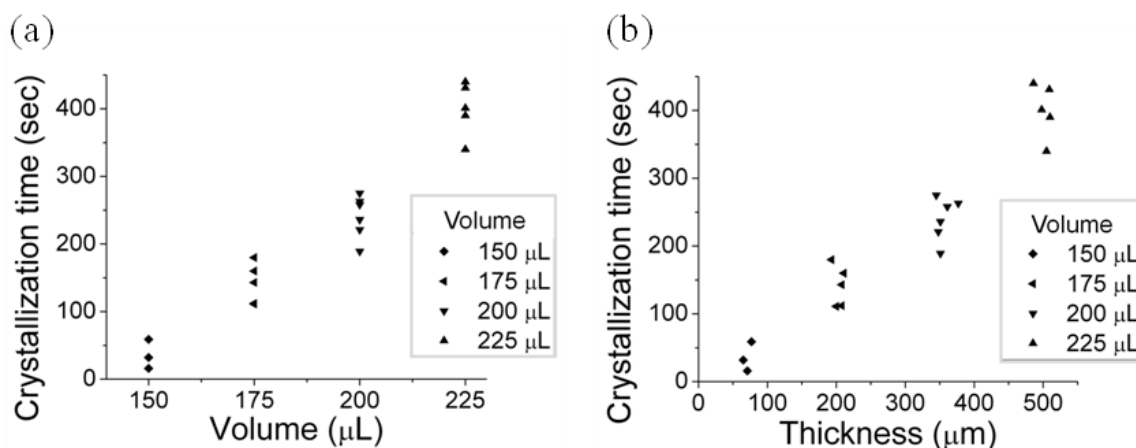


Fig. 3.5 Solution (a) volume and (b) thickness dependent crystallization time. Curves were obtained with 1.32 SS solution. Laser power is 1.0 W. Short glass tube was used as a container.

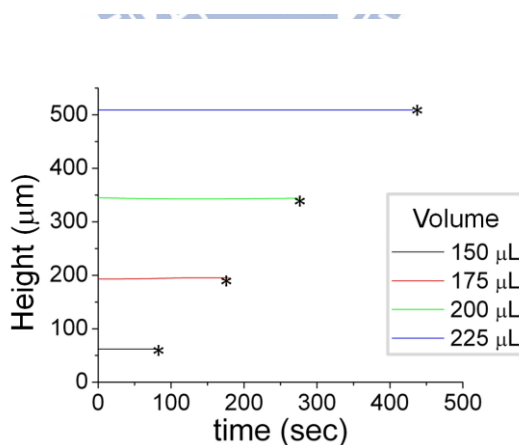


Fig. 3.6 Solution thickness dependence on crystallization time. Curves were obtained with 1.32 SS solution. Laser power is 1.0 W. Short glass tube was used as a container. Asterisk indicates crystallization occurred.

It implies that solution volume is correlated with mass flow of solute molecules. One key factor for laser trapping crystallization is most probably sufficient supply of molecules to the

focal spot by convection flow which induced by heat generation. Observed slowing of crystallization time probably related to slower or less effective convection flow and mass transfer in larger amount of solution which resulted in less effective condensation of the molecules to the focal spot of trapping laser. Local temperature and related mass transfer should be studied for this condition further.

3.3 Summary

We had examined CW laser trapping crystallization to obtain basic information of glycine crystallization under photon pressure by changing experimental parameters. We found power threshold around 600 mW for examined experimental condition. Lower crystallization probability at lower laser power range is attributed to less photon pressure which correct and pinned the molecules to the focal spot of the trapping laser. For laser-induced molecular assembly, 30 minutes irradiation of focused low power laser did not reach the critical concentration for nucleation. These results will be a great help for the comparison between CW and fs laser-induced crystallization in the following sections.

Volume dependence of laser trapping crystallization by focusing the CW laser at the air/solution interface is also examined. Necessary time for crystallization increased with increasing of solution volume. It shows linear increase in time. It implies that solution volume is correlated with local temperature elevation and mass flow of solute molecules in the solution.

4. Femtosecond Laser-Induced Crystallization

According to chapter 3, laser trapping crystallization of glycine with lower power CW laser is difficult. We cannot induce crystallization by CW laser below power threshold; for example less than 400 mW at examined conditions.

Femtosecond pulse lasers provide very high peak power that allow to access nonlinear processes within trapped particles, such as multi-photon absorption and harmonic generation [28]. Recent reports on the usage of fs pulse laser to trap semiconductor nanoparticles indicate that fs pulse laser can be more efficient trapping light source even at low power [29]. In this chapter we will use fs laser as a trapping light source in laser trapping crystallization of glycine and discuss the crystallization efficiency with different type of laser. We also discuss fs laser trapping crystallization mechanism.

4.1 Crystallization of glycine by femtosecond pulse laser

Figure 4.1 shows images taken during laser trapping crystallization of glycine which induced by focusing to the air/solution interface of saturated solution. After few minutes of femtosecond laser irradiation, the glycine crystal was generated at the focal point of trapping laser (Fig. 4.1). In previously reported amplified fs laser utilized crystallization method, we should see micrometer-size of cavitation bubble which induced by ablation of water. In the

examined power range of fs laser in this experiment, micrometer bubble or plasma emission was not observed during fs laser irradiation to the glycine solution. It is very unlike cavitation bubble-induced crystallization.

In addition to no bubble before crystal formation, generated crystal did not flow away from the focal spot. This result indicates that formed crystal is trapped by the photon pressure of irradiated fs laser. Therefore we can consider that observed crystallization is induced by exerted laser's photon pressure similar to CW laser trapping crystallization.

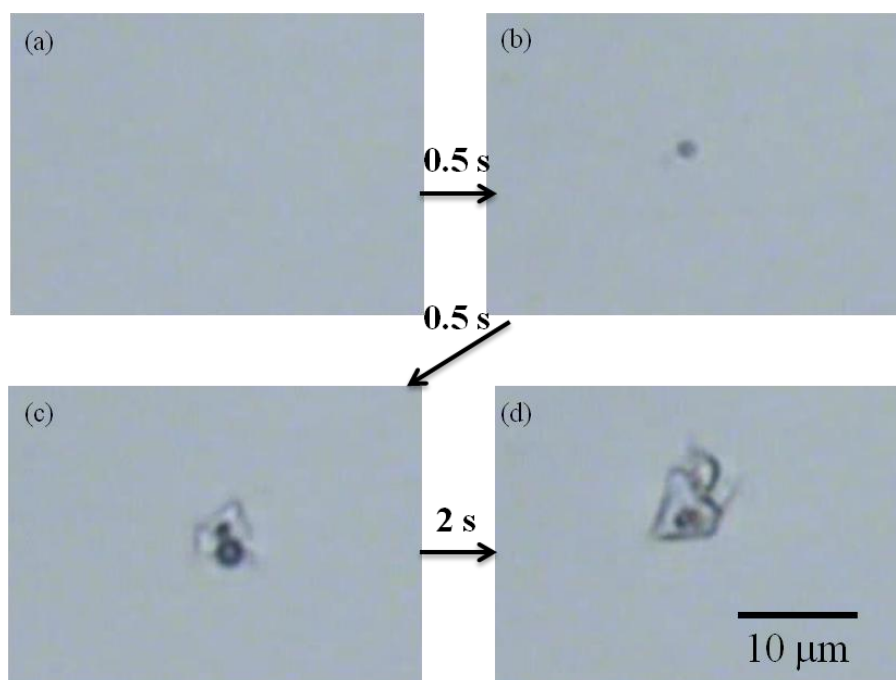


Fig. 4.1 Images taken during fs pulse laser induced trapping crystallization. Before fs laser irradiation (a), generated crystal (b), and trapped and grown crystal (c) and (d). Saturation degree of solution is 1.0 SS. Laser power is 600 mW. Similar to CW laser trapping crystallization, solution height did not change obviously but slightly decreased during fs laser irradiation to the air/solution interface.

Generated crystal was trapped at the focal point of the laser and quickly became larger to

tens of micrometer within a few to tens of seconds as shown in Fig. 4.1. It is first demonstration of fs laser pulse utilized laser trapping crystallization.

Figure 4.2 shows the comparison of the solution surface height change occurred by fs and CW laser irradiation. In contrast to faster height decrease induced by CW laser irradiation, the decrease induced by fs laser irradiation much slower and is similar to the decreasing without laser irradiation when we set the average power of CW (1064 nm) and fs (800 nm) lasers the same. It suggests that temperature elevation caused by fs laser irradiation is weaker than CW laser case. D₂O has smaller absorption coefficient at 800 nm than 1064 nm.

Therefore photothermal energy conversion due to the absorption of trapping laser should be less in 800 nm.

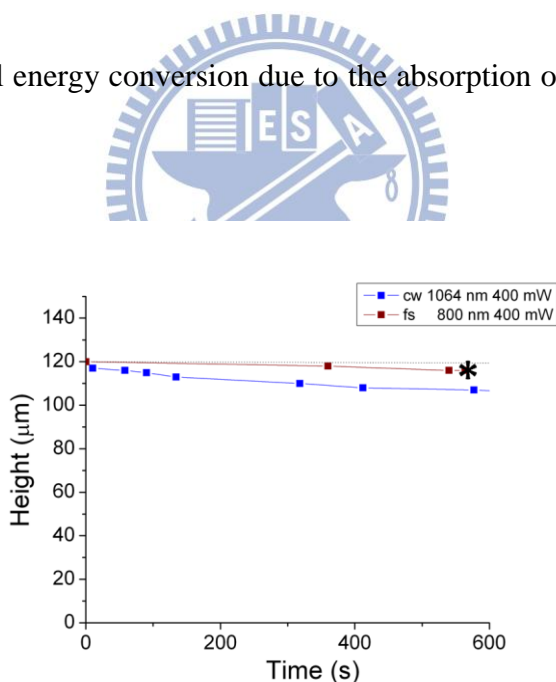


Fig. 4.2 Comparison of the solution height change under trapping laser irradiation. Both 1064 nm CW (blue line) and 800 nm fs (red line) lasers were set to the same average power (400 mW) and focused to the air/solution interface of the glycine solution. Asterisk indicates the moment crystallization occurred in 800 nm fs laser. Black dotted line in the figure is solution height change without laser irradiation.

4.2 Power dependence on fs laser trapping crystallization

As we see in the above results, crystallization was achieved due to the laser trapping. Photon pressure for optical trapping should be proportional to the laser intensity, therefore, it is expected to see the laser power or energy threshold for the crystallization. To find out the threshold energy of fs laser-induced crystallization, we check the power dependence by changing trapping laser power from 100 to 600 mW. As well as CW laser trapping case, we limited the experiment time to 30 min.

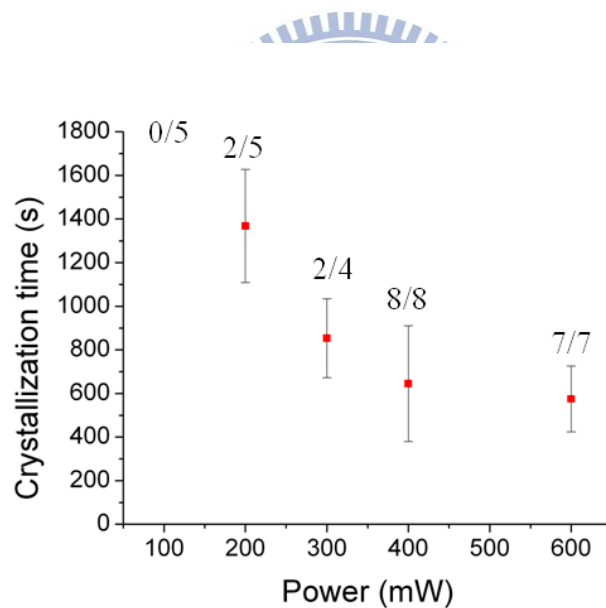


Fig. 4.3 Power dependence of crystallization time of fs laser trapping crystallization. 100, 200, 300, 400, and 600 mW fs laser was applied. Observation time is 30 min. Saturation degree of solution is 0.9 SS.

Figure 4.3 shows the distribution of the time required to see the crystallization. Crystallization probability, namely whether we can see or not the crystallization within 30

min, of examined laser powers is mentioned in the figure. We could induce the crystallization above 200 mW under examined saturation degree of 0.9 SS and 30 min of observation time. Crystallization time became longer with decreasing of trapping laser power. We could make crystal in all experiment above 400 mW, however, crystallization probability decreased with decreasing of trapping laser power and could not induce crystallization at 100 mW. This result indicates that the threshold energy of fs laser-induced crystallization is 200 mW. An energy threshold of fs laser trapping crystallization is estimated to 2.5 nJ/pulse from the operation frequency of the laser which is 80 MHz.

4.3 Focus position dependence on fs laser trapping crystallization

We have observed irradiation position dependent trapping behavior change in laser trapping assembling of some amino acids, polymer and proteins. Actually, we need to focus the trapping laser to the air/solution interface to achieve crystallization by trapping and no crystallization can be seen by focusing to the different position such as inside of the solution or glass/solution interface. Thus we examined focus position dependence on fs laser trapping crystallization with focusing to the air/solution interface, inside of the solution, and the glass/solution interface. Figure 4.4 shows schematic drawing of irradiation position and results obtained by focusing to these positions. Crystallization was achieved only by focusing fs pulses to the air/solution interface. Focusing a trapping laser in the solution and

to the glass/solution interface could not form crystal even we irradiate the laser more than 30 min. It is quite similar with CW laser trapping crystallization. This result implies that the air/solution interface should have some sort of important role for the laser trapping crystallization.

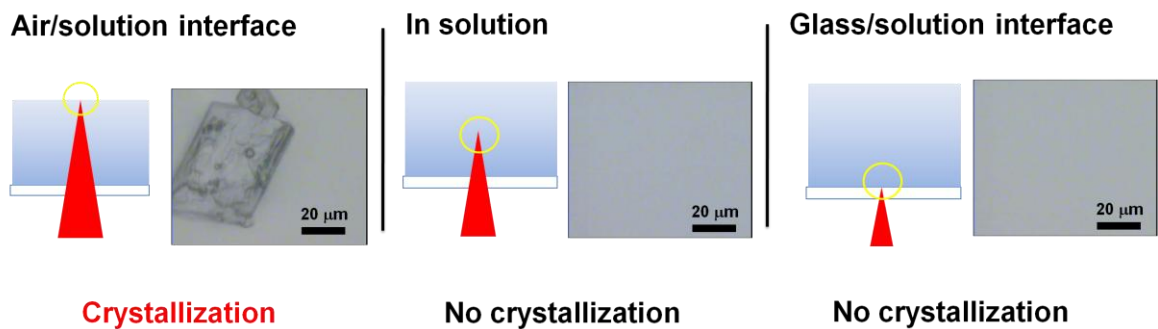


Fig. 4.4 Focus position dependence on fs laser trapping crystallization. Crystallization occurred only focusing to the air/solution interface as well as CW laser trapping crystallization. Saturation degree of solution is 0.9 SS. Laser power is 600mW.

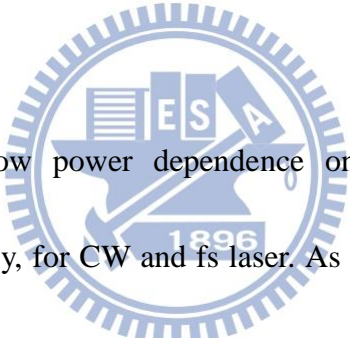


4.4 Comparison between fs and CW laser trapping crystallization

Figure 4.5 shows the snapshots of crystallization process obtained from fs (Fig. 4.5a) and CW (Fig. 4.5b) laser trapping crystallization by focusing to the air/solution interface. Both trapping method can generate crystal from the focal spot of trapping laser. High positional controllability is one of the advantages of laser trapping crystallization. This result reveals not only CW but also fs laser trapping crystallization method also similarly can provide high spatial controllability.

Typically CW laser trapping can form a crystal with 1200~1400 sec after starting trapping

laser irradiation at 600 mW under examined experimental conditions. Formed crystal was trapped to the focal position of the CW laser and grows to several tens of micrometer in several minutes. On the other hand, fs trapping gives crystal within much shorter time even experimental condition was the same as CW case; here average laser power was the same 600 mW. Furthermore generated crystal grew quite faster than CW case under trapping to the laser spot as depicted in Fig. 4.6. It became more than ten micrometer within 1 ~2 min as shown in Fig. 4.6b, meanwhile grown size of the crystal trapped by CW laser was less than 5 μm . Compare with CW laser case, fs laser-induced crystallization showed faster crystal growth.



Figures 4.7a and 4.7b show power dependence on crystallization probability and crystallization time, respectively, for CW and fs laser. As we can see in Fig. 4.7a clearly, fs laser trapping gives much higher crystallization probability and shorter crystallization time than that of CW laser. Crystallization probability and crystal generation time for both lasers under different powers were summarized in Table 4.1. Optical trapping force for laser trapping proportionally changes with the laser intensity change. Higher crystallization probability with shorter crystallization time implies fs laser can induce the crystallization more efficiently than CW laser. Based on the conventional crystallization mechanism, crystallization probability and crystal formation speed will change by local concentration change where the crystal appeared, namely it suggests that rapid elevation of the

concentration around the laser spot was achieved effectively. According to higher probability and shorter crystallization time, fs laser trapping crystallization can be considered as more efficient and powerful than CW trapping crystallization.

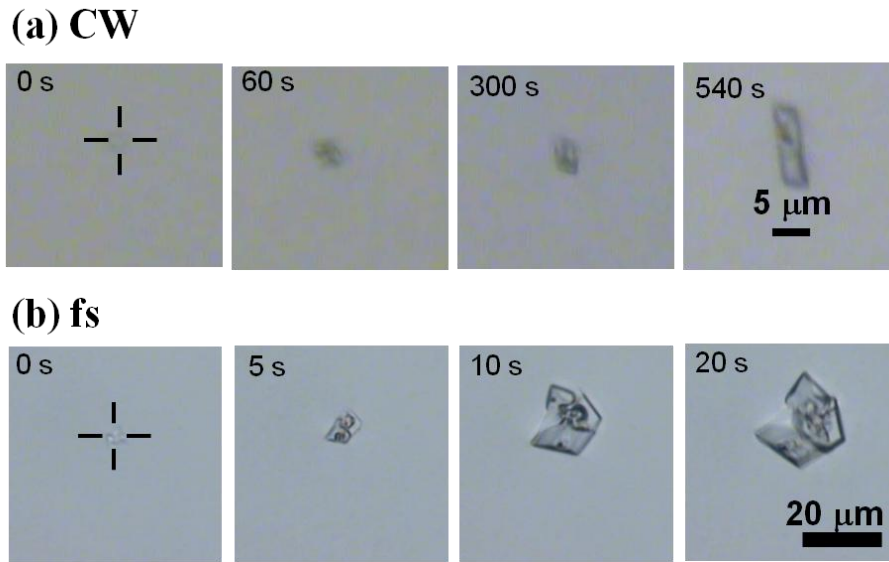


Fig. 4.5 Snapshots of laser trapping crystallization process induced by (a) CW and (b) fs laser. Average laser power of both lasers were 600 mW. Saturation degree of solution is 0.9 SS.

Table 4.1 Crystallization probability and time for different trapping laser power of fs and CW laser trapping crystallization.

| | fs | | | | | CW | |
|---------------------------------|-----|----------|---------|---------|---------|-----|---------|
| Power (mW) | 100 | 200 | 300 | 400 | 600 | 400 | 600 |
| Probability | 0/5 | 2/5 | 2/4 | 8/8 | 7/7 | 0/5 | 2/4 |
| Crystallization time (s) | — | 1368±259 | 853±181 | 645±265 | 575±151 | — | 1303±45 |

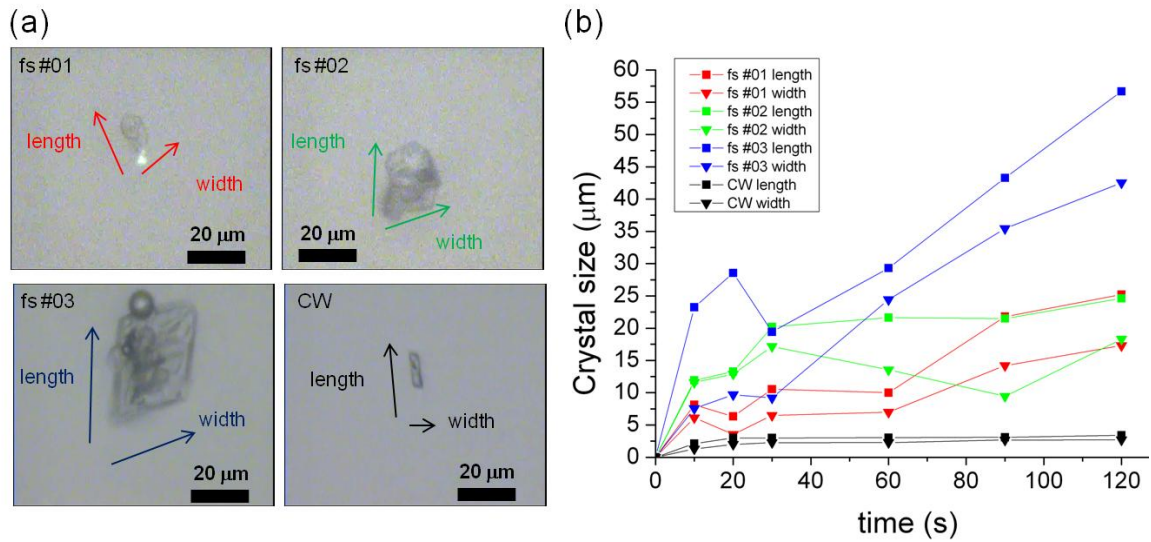


Fig. 4.6 (a) Crystal pictures and crystal size definition, and (b) crystal growth rate by irradiating fs and CW lasers. Laser power is 600 mW. Saturation degree of the solution is 0.9 SS.

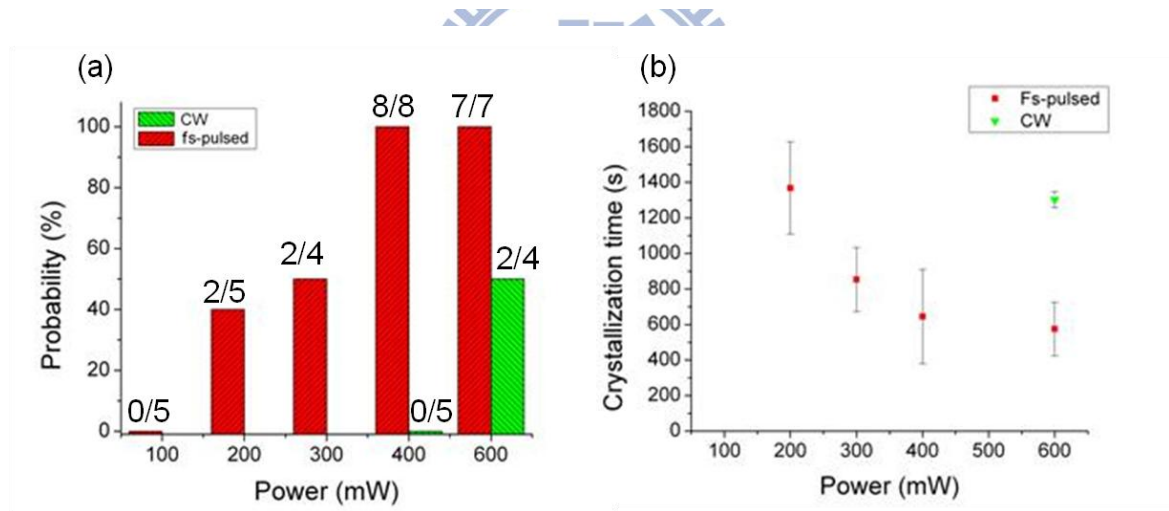
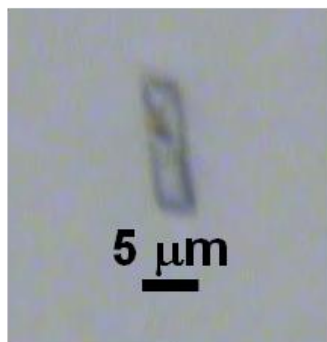


Fig. 4.7 (a) Crystallization probability and (b) crystallization time induced by fs and CW lasers. Green and red markers correspond to CW and fs laser, respectively. Examined laser powers are 100, 200, 300, 400, 600 mW. Saturation degree of the solution is 0.9 SS. Observation time is 30 min.

(a) CW



(b) fs pulse

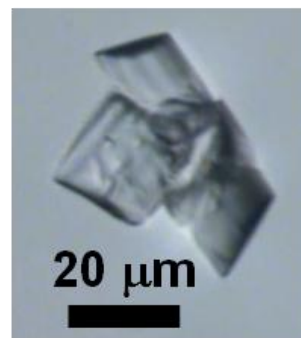


Fig. 4.8 Pictures of (a) CW laser-induced single glycine crystal and (b) fs laser-induced polycrystal. In fs case, crystal growth and damage on the crystal surface simultaneously took place.

Although fs laser trapping crystallization is more efficient than that by CW laser, there is one drawback in this method: crystal obtained in fs trapping is not a single crystal. As shown in Fig. 4.8a, CW laser trapping could form one single crystal, on the contrary we typically observed polycrystal after crystal growth under fs trapping. Quickly formed crystal in fs trapping will be trapped at the focal point and be ablated due to high peak energy of fs laser. Thus generated seed crystal was divided into small pieces and trapped again, grew under high concentration which induced by optical force of fs laser, and eventually became polycrystal. Although we cannot obtain a single crystal in fs laser trapping crystallization, this method showed the advantages such as higher crystallization efficiency compare to CW laser. Therefore it is worth finding the solution for single crystal formation with femtosecond laser and we will examine it in next chapter.

4.5 Discussion

We found that focused fs laser to the air/solution interface could induce crystallization with higher crystallization efficiency compare to CW laser. Here we discuss about the possible mechanism of fs laser-induced crystallization. Base on the photon number in a short time, we will make a comparison between different optical crystallization methods with low energy fs, amplified fs and CW lasers.

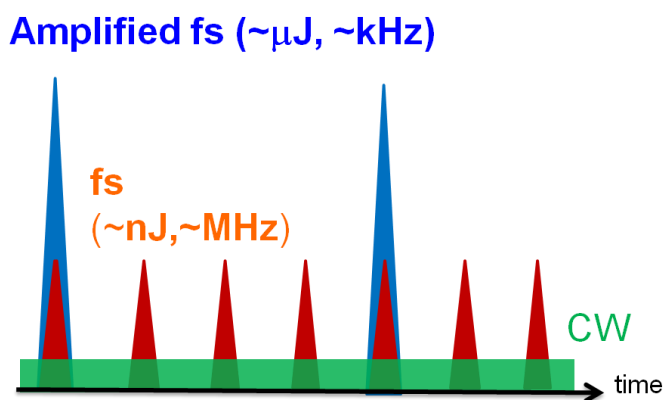


Fig. 4.9 Illustration of laser energy comparison of low energy fs laser, amplified fs laser, and CW laser.

4.5.1 Trapping by low energy fs laser operated at high repetition rate

Here we consider a possible mechanism of femtosecond laser-induced crystallization in glycine solution. Because the trapping force on one glycine molecule is not enough to overcome the Brownian motion in solution. Therefore, laser-induced molecular assembly formation by trapping single glycine molecules is impossible. It has been reported that the presence of small liquid-like clusters of glycine under a supersaturated condition [56]. Locally induced concentration elevation is considered due to the gathering of glycine

clusters around the focal spot by photon pressure [21]. High intensity of laser light at the focal spot can accumulate glycine clusters, and the density of the trapped clusters proportionally increases with the increase of the laser power.

Unlike CW laser case, intense electric field is provided with very short pulse intervals; for example oscillator's 80 MHz repetition rate provides 150 fs laser pulse at every 12.5 ns. In the case of neutral nanoparticles (NPs), NPs trapped by fs laser cannot escape and release themselves from the trapping site by diffusion during the interval between two laser pulses. Diffusion coefficient of a polystyrene NP in water is in the order of $\sim 10^{-10} \text{ m}^2 \text{ s}^{-1}$ for 57 nm diameter polystyrene NP [65]. Diffusion distance of the NPs within 12.5 ns is merely 4 nm^2 which is much smaller than the focal spot size ($\sim 10^6 \text{ nm}^2$). It indicates that trapped NP by fs pulse train cannot easily escape from the focal volume by diffusion as shown in Fig. 4.10a and 4.10b. Next pulse arrived in short duration, i.e. 12.5 ns, will collect other particles and the concentration of the particles at the focal spot will be increased more. Again, the particles cannot diffuse much during pulse interval (Fig. 4.10c and 4.10d), and next pulse induce further accumulation of the particle as shown in Fig. 4.10e. It will be repeated until effective trapping volume is filled with particles. Particle concentration can be drastically increased with repeating fs laser trapping.

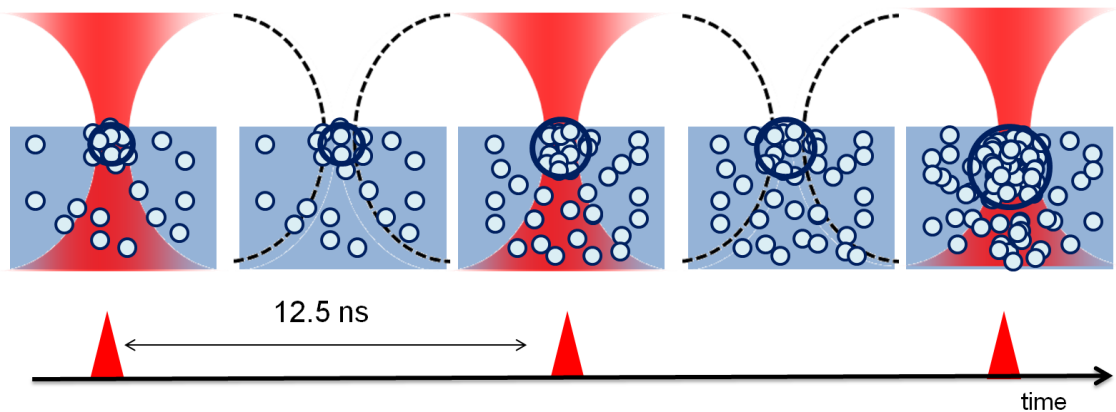


Fig. 4.10 Schematic drawing of femtosecond laser trapping induced accumulation of molecule at the focal spot.

As well as polystyrene NPs, glycine clusters which are collected and trapped by photon pressure of fs trapping laser can be accumulated to the focal spot with high repetition rate operation. Additionally zwitterionic form of glycine in neutral aqueous solution enhances the interaction of molecules/cluster and prohibits the release of the clusters from the trapping volume. Thus cluster density at the focal spot will be further increased by photon forces and local high concentration area can be formed. Concentration of glycine will overcome the threshold for the phase transition to form crystal by trapping and eventually crystallization becomes possible.

4.5.2 Comparisons of fs laser trapping crystallization and amplified fs laser-induced crystallization

Amplified fs laser-induced crystallization can form crystals of molecules such as glycine

and lysozyme from their supersaturated solution by focusing an amplified fs laser [49].

Intense fs laser focusing to the aqueous solution induce optical breakdown of water. Pulse energy and repetition rate dependences show that the frequency of cavitation bubble generation induced by multiphoton absorption of water. The mechanism of amplified fs laser-induced crystallization is mainly attributed to the local concentration change around the cavitation bubble. Necessary condition to realize amplified fs laser-induced crystallization of glycine is supersaturated glycine solution. In the case of low saturation condition, it is difficult to induce crystallization. Meanwhile, low energy fs laser can induce local high concentration area by focusing to the air/solution interface and crystallization is also possible even unsaturated solution.

Peak power of a single pulse of low energy femtosecond laser is 7.5 nJ, and the energy density is 0.81 Jcm^{-2} , at 600mW and 80 MHz. Energy density in our fs laser experiment is much smaller than threshold energy of optical breakdown in water ($F_{th} \sim 5.64 \text{ Jcm}^{-2}$) [66] and cannot induced the breakdown of water. In actually we never observed microbubble, which play a key role for amplified laser-induced crystallization, during fs laser irradiation. This experimental fact denies that crystallization due to the microbubble formation in our experiment, and thus we can consider that the mechanism between amplified fs laser- and low energy fs laser-induced crystallization are different. Crystallization though local high concentration due to the photon pressure should be more reasonable for our experiments.

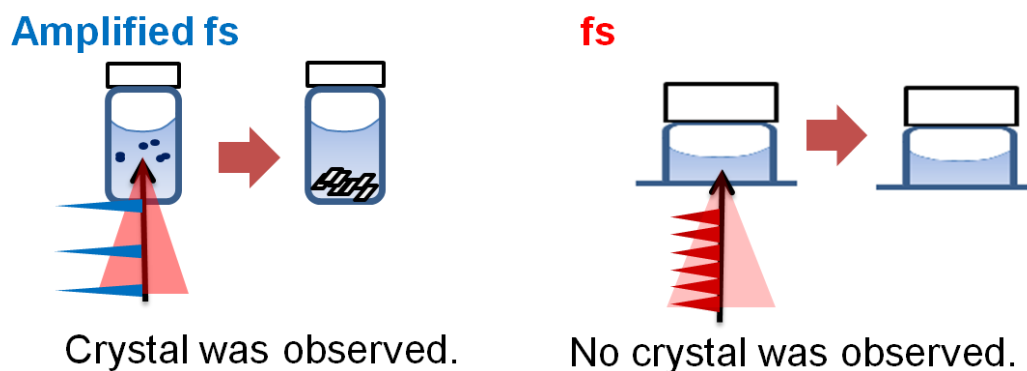


Fig. 4.11 Schematic drawing of focused amplified fs laser and low energy fs laser focused into the solution. Micrometer-size cavitation bubble plays a key role in amplified fs laser. Supersaturated glycine solution is necessary in the amplified fs laser case.

4.5.3 Comparisons of fs and CW trapping crystallization

As we mention before, fs laser-induced crystallization showed a higher efficiency of nucleation than CW laser case. Efficient crystallization by fs pulse laser is considered due to efficient trapping of the molecules/clusters by stronger radiation pressure. Number of photons per second is 2.01×10^{23} for laser pulses with an average power of 600 mW and pulse width of 150 fs. It is almost five orders of magnitude higher than the number of photons of CW laser in 150 fs (2.41×10^{18}) for the same laser power. Higher optical trapping efficiency of pulsed laser can be attributed to the difference of the number of photons between fs and CW [67]. Although no trapping force exists during the interval of two laser pulses, glycine clusters cannot easily escape by diffusion from the focal spot as we mention above.

4.6 Summary

We succeeded to crystallize glycine by applying fs laser pulses for the first time in the world. fs laser-induced crystallization showed higher crystallization probability and shorter crystallization time under the examined power range and concentration than CW laser trapping. We think that the crystallization is caused by laser trapping of glycine cluster since we can see the trapping of generated crystal. Faster crystal growth observed for trapped crystal also suggests the formation of locally high concentration area around focal spot. However, high energy in one pulse cause the ablation of generated crystal and it became polycrystal eventually. It should be necessary to find suitable condition to form single crystal.

We discuss the possible mechanism of fs laser trapping crystallization by comparing fs laser, amplified fs laser, and CW laser induced crystallizations. Examined powers in fs laser trapping crystallization are too low to induced breakdown of water and generate cavitation bubble which induces crystallization in amplified case. The mechanisms between amplified fs laser- and fs laser-induced crystallization are different. Crystallization though local high concentration seems more reasonable to explain our crystallization. Higher optical trapping efficiency of pulsed laser can be attributed to the difference of the number of photons between fs and CW.

5. Single crystal formation by a combination of fs and CW lasers

Although formed crystal can be trapped and stably grow without damage under CW laser trapping crystallization, probability of crystallization by using low power CW laser is not so high as we mentioned in chapter 3. On the other hand, fs laser can induce crystallization more efficiently under the same average power, however generated crystal easily became a polycrystal due to the ablation by continuous fs pulse laser irradiation. Both methods have advantages and disadvantages. Here we propose and demonstrate fs and CW combined new laser trapping method which enable the fabrication of single crystal with higher crystallization probability, better efficiency, faster crystallization, and better temporal controllability.



5.1 Femtosecond laser-induced crystallization: Approach 1, fs for nucleation and growth without laser irradiation

The idea for single crystal formation with applying femtosecond laser is simple: do not let fs laser damage the formed crystal. In the first approach, we irradiate fs laser until we observe the generated crystal and after observing the generation of the crystal we turn off fs laser immediately, and wait for the crystal becomes big. Figure 5.1 shows the sequential pictures of crystal formation during fs irradiation and growth after turn off the laser (Fig. 5.1a), and schematic representation of laser on/off timing. Trapping fs laser was focused to

the air/solution interface to induced crystallization and saturation degree of solution was 1.0 SS. When the glycine crystal generation was confirmed, fs laser irradiation was stopped immediately to prevent the laser ablation on the crystal. Even after stopping fs laser irradiation, crystal grew spontaneously. It is probably due to induced high concentration region by fs laser trapping. Immediate termination of fs laser after finding of the crystal greatly decreased the fs laser ablation provability and, as a result, we can obtain single crystalline solid with higher probability compared to previous results shown in chapter 4.

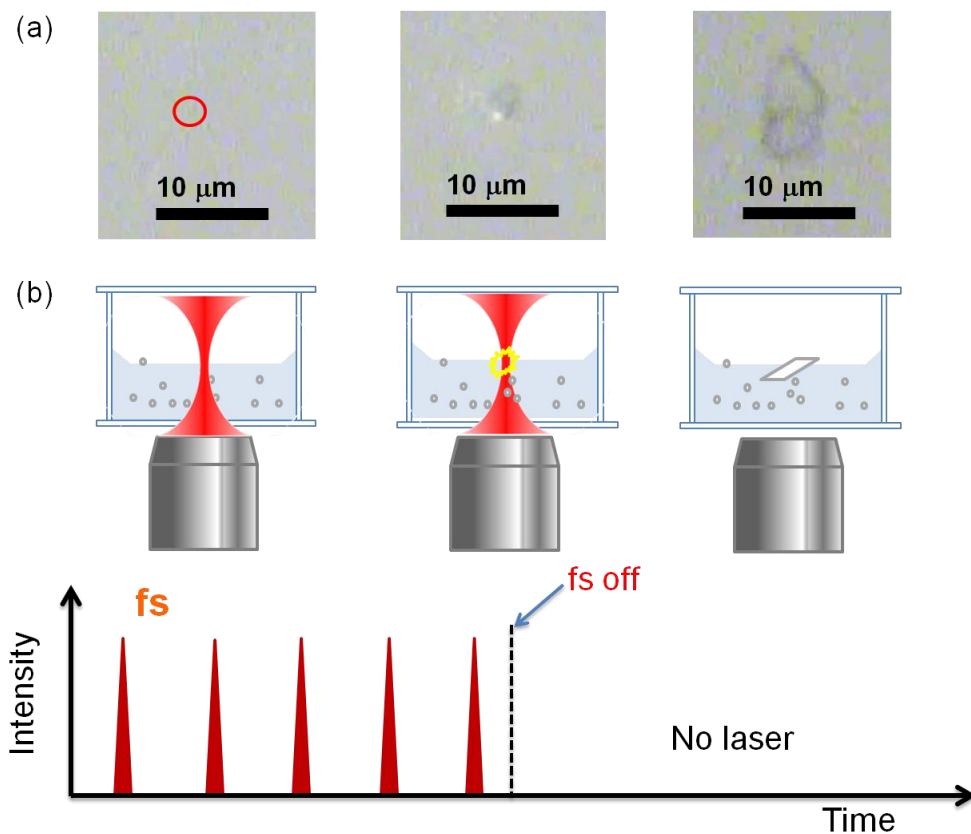


Fig. 5.1 (a) Sequential pictures obtained during fs laser trapping crystallization and crystal growth without laser irradiation and (b) schematic drawing of femtosecond laser-induced crystallization by terminating fs laser irradiation after observing crystal generation. fs laser power is 400 mW. Saturation degree of solution is 1.0 SS.

In order to obtain a large crystal from the laser trapping generated crystal, we incubated formed crystal in sample chamber with evaporating the solvent slowly. Figure 5.2 shows the schematic drawing of solvent evaporation process for obtaining a millimeter-size glycine crystal. After confirming crystal generation and growth of it more than several tens of μm , a cap of the glass chamber was opened and left a small space for the solvent evaporation forcing solvent evaporated slowly. Concentration of the whole solution increase gradually and the crystal grow to a millimeter-size as shown in Fig. 5.3. This method was used for making the crystal large in all latter crystallization experiments.

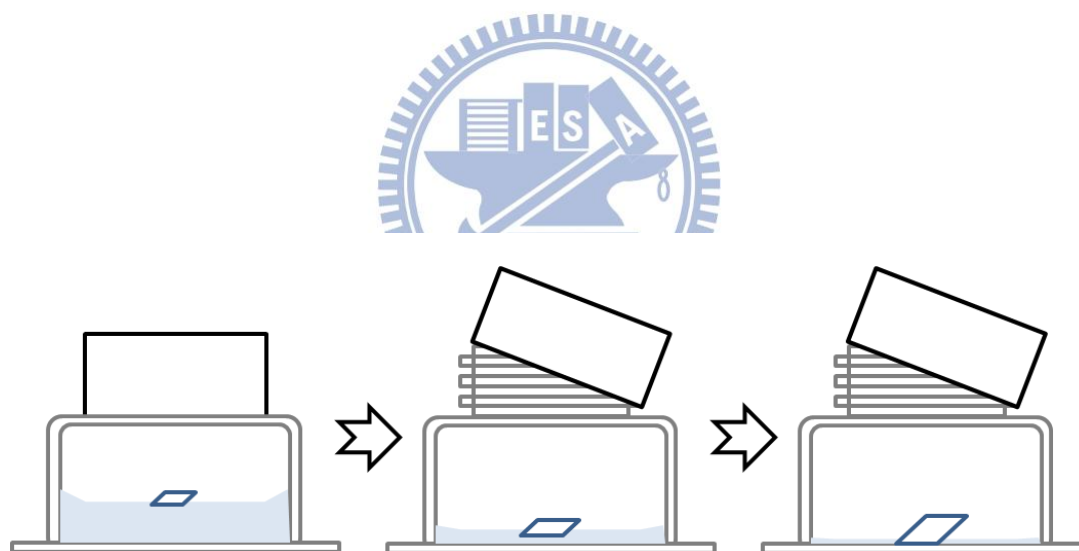


Fig. 5.2 Schematic drawing of solvent evaporation process to obtain a millimeter-size crystal.

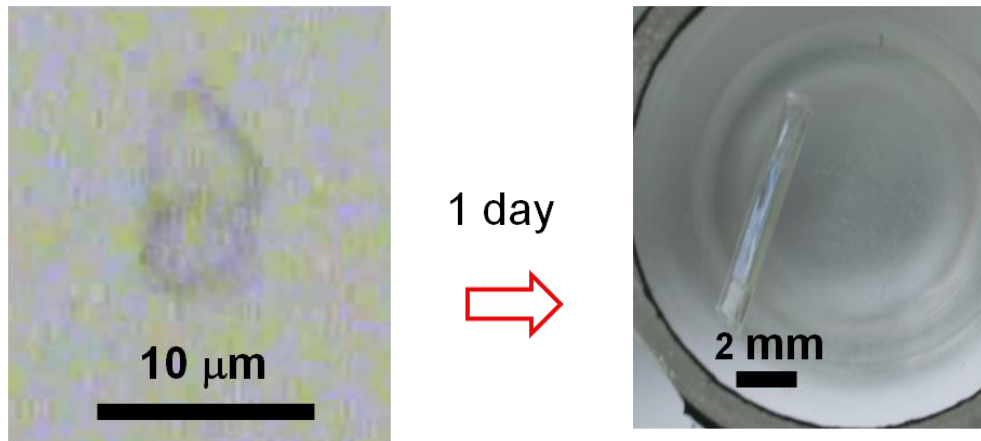


Fig. 5.3 Pictures of the obtained millimeter-size single crystal of femtosecond laser-induced crystallization without further irradiation.

By waiting until the crystal became large to millimeter-size, grown crystals were single crystal, but the success ratio of obtaining a large crystal after solvent evaporation process was low. The problem we faced here was disappearance of the crystal. Sometimes we cannot observe glycine crystal one day after in this experiment. Formed crystal flow away from the focal spot of the laser without trapping laser, therefore we cannot confirm the crystal growth to the sufficient size. Additionally due to the trapping force from fs laser, glycine cluster were concentrated around the laser focal spot. Here we used relatively low saturation degree solution (S.S. = 1.0) compare to previous study of laser trapping crystallization (S.S. = 1.32) to prevent unexpected crystallization which is not due to the laser irradiation [51]. Therefore generated crystal can be dissolved into solution if the crystal will flow into lower concentration area. Figure 5.4 shows the hypothesis of the dissolution process of formed

crystal. After the laser trapping experiment, low concentration region of the solution is unsaturated. Once the generated crystal flow to the low concentration region, it would dissolve easily. We cannot make sure the crystal from the trapping site still existing or not after the experiment. Due to the uncertainty of this method, we can obtain less than three large crystals out of ten laser trapping generated crystals. This method is not suitable for large single crystal fabrication because of its low success ratio.



Fig. 5.4 Schematic drawing of dissolution of formed crystal in unsaturated region. Deep blue means the high concentration area induced by trapping laser.



5.2 Femtosecond laser-induced crystallization with further CW laser irradiation

Utilization of a 400 mW CW laser cannot induce crystallization, but it can trap a crystal and make the crystal larger. This information indicated that we can apply this characteristics of weak laser on trapping of crystal and crystal growth. Figure 5.5 shows the sequential process of method 2. Same with method 1, the first step is utilizing fs laser to induce

crystallization of glycine. When the generation of small seed crystal was observed, fs laser was turned off immediately and turn on the CW laser. Focusing CW laser ($\lambda = 1064 \text{ nm}$) to the crystal for several minutes make crystal large. Laser was irradiated at the air/solution interface. From the previous experience, we knew the importance of laser trapping. Without the application of laser trapping, it is difficult to monitor the crystal growth process. It is better to prepare larger crystal for the solvent evaporated crystal enlargement process since if the crystal will not easily dissolve if the crystal is sufficiently large. Usually safe size for stable crystal growth during evaporation process is more than $10 \mu\text{m}$.

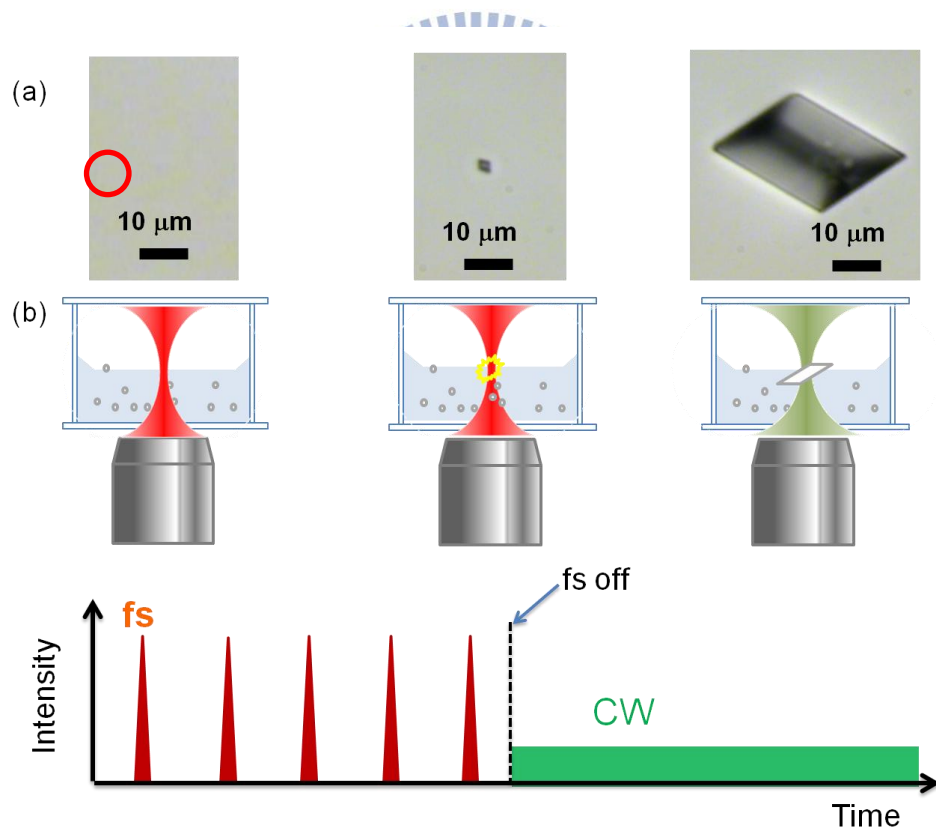


Fig. 5.5 (a) Pictures of the crystallization and (b) schematic drawing of fs laser-induced crystallization with further CW laser irradiation. Power of both fs and CW laser is 400 mW. Saturation degree of solution is 1.0 SS.

Figure 5.6 shows the crystallization of fs laser-induced crystallization with further CW laser irradiation. Generated seed single crystal can be enlarged by CW laser trapping as seen in the first and second panel of Fig. 5.6. Single crystal of glycine was observed after solvent evaporation process in the third panel of Fig. 5.6. With CW trapping laser, the formed crystal was grown into several tens of micrometer. This result suggested that large crystal more than tens of micrometer can survive during the solvent evaporation process. Compare with previous method without CW laser irradiation, we could make one large single crystal (millimeter) with higher success ratio (more than 80%) after solvent evaporation in method

2.

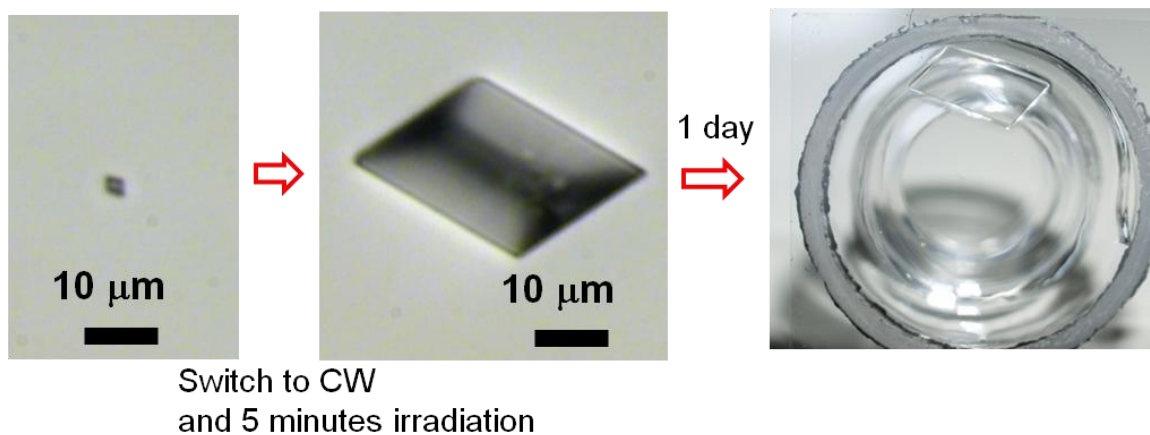


Fig. 5.6 Pictures of the obtained millimeter-size single crystal of femtosecond laser-induced crystallization with further continuouswave laser irradiation.

5.3 Low power CW laser trapping crystallization with a short time irradiation of fs laser

In actually, perfect single crystal formation rate in method 1 and method 2 was not so high. Small crystal or damage remains on the resulting large crystal. We consider above mentioned two crystallization methods are similar in that both of them are crystallized by femtosecond laser pulse. This crystallization process cannot avoid laser ablation entirely. Base on this, we introduce single crystal formation method 3. The idea for preventing the laser ablation is applying fs laser to induce nucleation and immediate stop of fs pulse irradiation. From previous results showed in chapter 3, only with low power (400 mW) CW laser cannot induce crystallization within 30 minutes, it is suggested that concentration at the focal point is not high enough for crystallization, but we still can apply its photon pressure on collecting molecules. Figure 5.7 shows the design of this experiment, we prepared local high concentration by CW and fs laser simultaneously, and crystallization by only CW laser, to see if the low power laser can crystallize in this condition. fs laser was turn off before crystal appear.

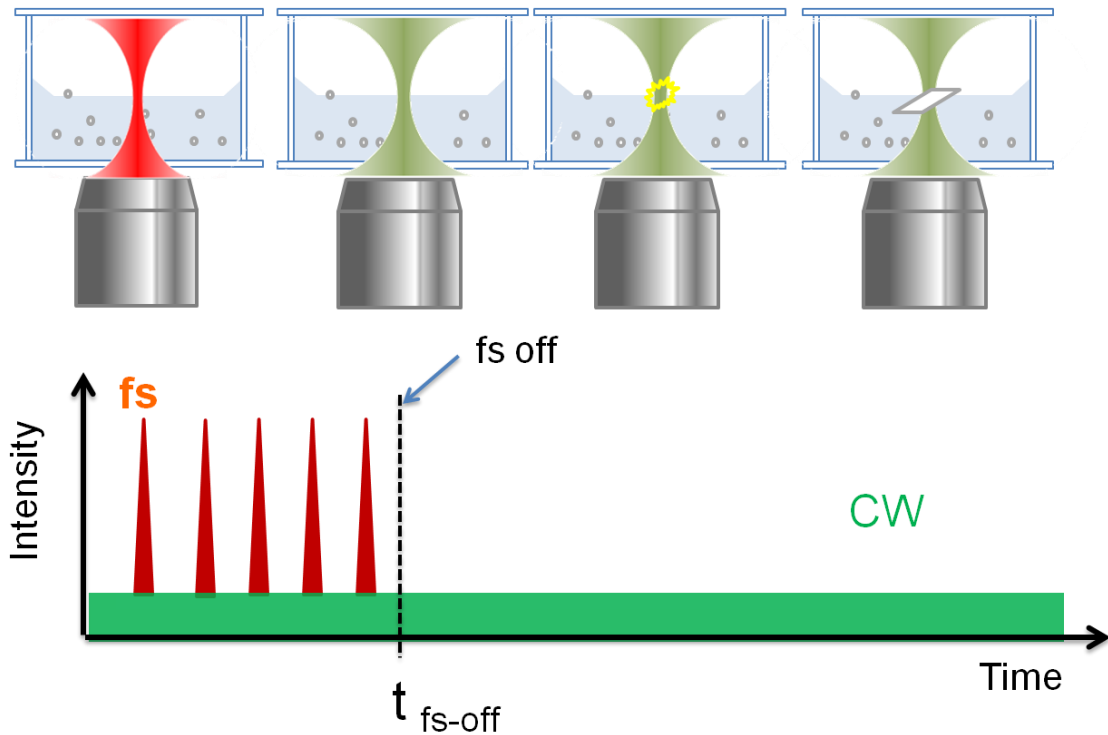


Fig. 5.7 Schematic drawing of low power CW laser trapping crystallization with a short time irradiation of fs laser.

It should be noted that applied laser power of CW laser is too low to generate crystal under examined condition. Both lasers were irradiated at the air/solution interface. Compare with previous single crystal formation method, this experiment condition is not simple. Before doing the experiment, we should clarify some information. One point we have to notice is choosing the suitable power of CW laser which cannot induce crystallization within the setting time (30 minutes). As we mentioned in chapter 3, CW laser cannot induce crystallization within limitation time when laser power is less than 400 mW. So we selected power at 200 and 400 mW for low power CW laser trapping crystallization experiment.

To avoid laser ablation on the crystal, we cannot give a long irradiation time of fs laser.

But if the fs laser irradiation time is not long enough, focused fs laser cannot induce molecular assembly efficiently. For this reason, set a suitable irradiation time of fs laser is important. Figure 5.8b shows the distribution of crystallization time by focusing CW and fs laser simultaneously. Laser trapping crystallization is stochastic phenomenon as well as conventional crystallization and impossible to determine crystallization timing. From the necessary crystallization time of two lasers induced crystallization, we can know the maximum acceptable fs laser irradiation time until crystal generation. For this experiment, we set the fs laser irradiation time as 5 minutes and 10 minutes for 400 and 200 mW of CW laser, respectively.

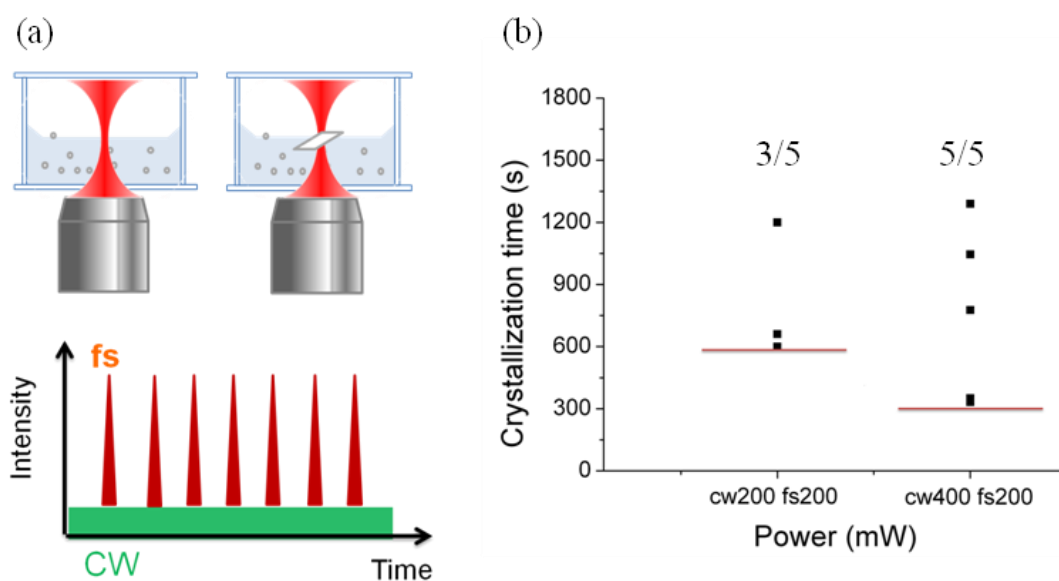


Fig. 5.8 (a) Schematic drawing of laser irradiation manner in simultaneous fs and CW laser irradiation. (b) Laser trapping crystallization of glycine by focusing 1064 nm cw and 800 nm fs laser simultaneously. The limited experiment time is 30 minutes. Saturation degree of solution is 1.0 SS.

Figure 5.9b shows the success probability and crystallization time of this experiment. Crystallization probabilities in both experimental conditions are summarized in table 5.1. With 5 minutes of simultaneous fs and CW, and further CW laser irradiation, induce crystallization when CW is 400 mW. In contrast, we could not obtain the crystal with 200 mW CW laser.

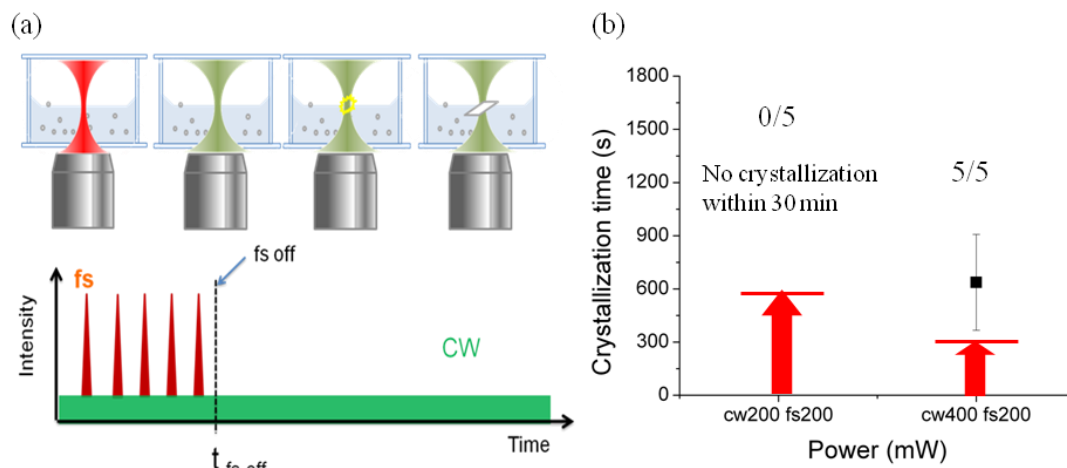


Fig. 5.9 (a) Schematic drawing of laser irradiation manner in method 3. (b) Success probability and crystallization time of low power CW laser trapping crystallization with a short time irradiation of fs laser. The red arrow means fs laser irradiated. The limited experiment time is 30 minutes. Saturation degree of solution is 1.0 SS.

Table 5.1 Setting fs laser irradiation time and crystallization probability under different combination of CW and fs lasers

| | | |
|--------------------|-----|-----|
| CW (mW) | 200 | 400 |
| fs (mW) | 200 | 200 |
| t_{fs-off} (min) | 10 | 5 |
| Probability | 0/5 | 5/5 |

Crystallization pictures of low power CW laser trapping crystallization with a short time irradiation of fs laser is shown in Fig 5.10. Crystallization was carried out under 200 mW fs and 400 mW CW laser power. Here, fs laser was not irradiated when the crystal generated. Crystallization process was similar to CW laser trapping crystallization. Laser ablation on the crystal was entirely avoided in this experiment. Without damage on the crystal surface, single crystal could be obtained. After solvent evaporation and growth, we could obtain a millimeter-size large single crystal.

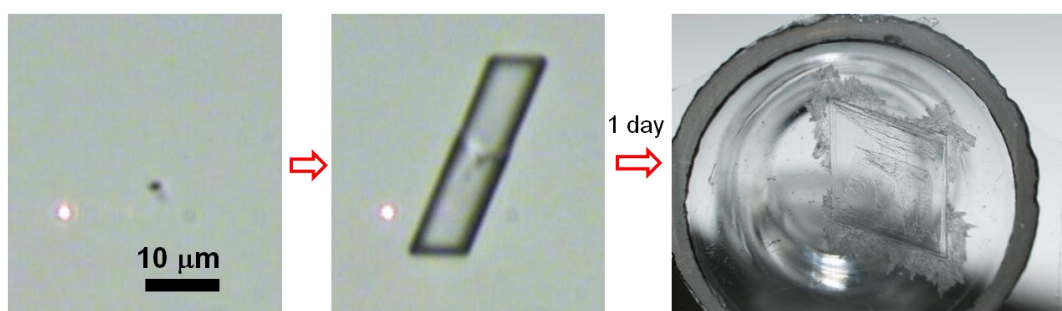


Fig. 5.10 Pictures of the crystallization of low power CW laser trapping crystallization with a short time irradiation of fs laser.

5.4 Temporal control of crystallization by millisecond exposure time of fs laser

Single crystal formation method 4 is shown in figure 5.11. After forming local high concentration area by focusing CW laser at the air/solution interface, and then give a short time fs laser irradiation at the high concentration region to see if short time fs laser can induce crystallization of glycine. In this experiment, we first irradiate CW laser and then irradiate very short time a fs laser to persuade a crystallization. A 200 mW of CW laser was irradiated for 25 minutes for preparing a local high concentration at the focal position. We did not observe crystal generation during CW laser irradiation as shown in Fig. 5.11a left panel. Then CW laser was tentatively cut and irradiate fs laser just only for 50 ms, and turn on CW laser again. Here we used 200 mW of fs laser. After irradiation of fs laser, singular crystal was formed spontaneously within a few to a few tens of seconds (Fig. 5.11a middle panel). CW laser trapped generated singular crystal at the focal spot of trapping laser and the crystal grew into a larger size as seen in Fig. 5.11a right panel. After solvent evaporation, we could obtain a millimeter-size large single crystal.

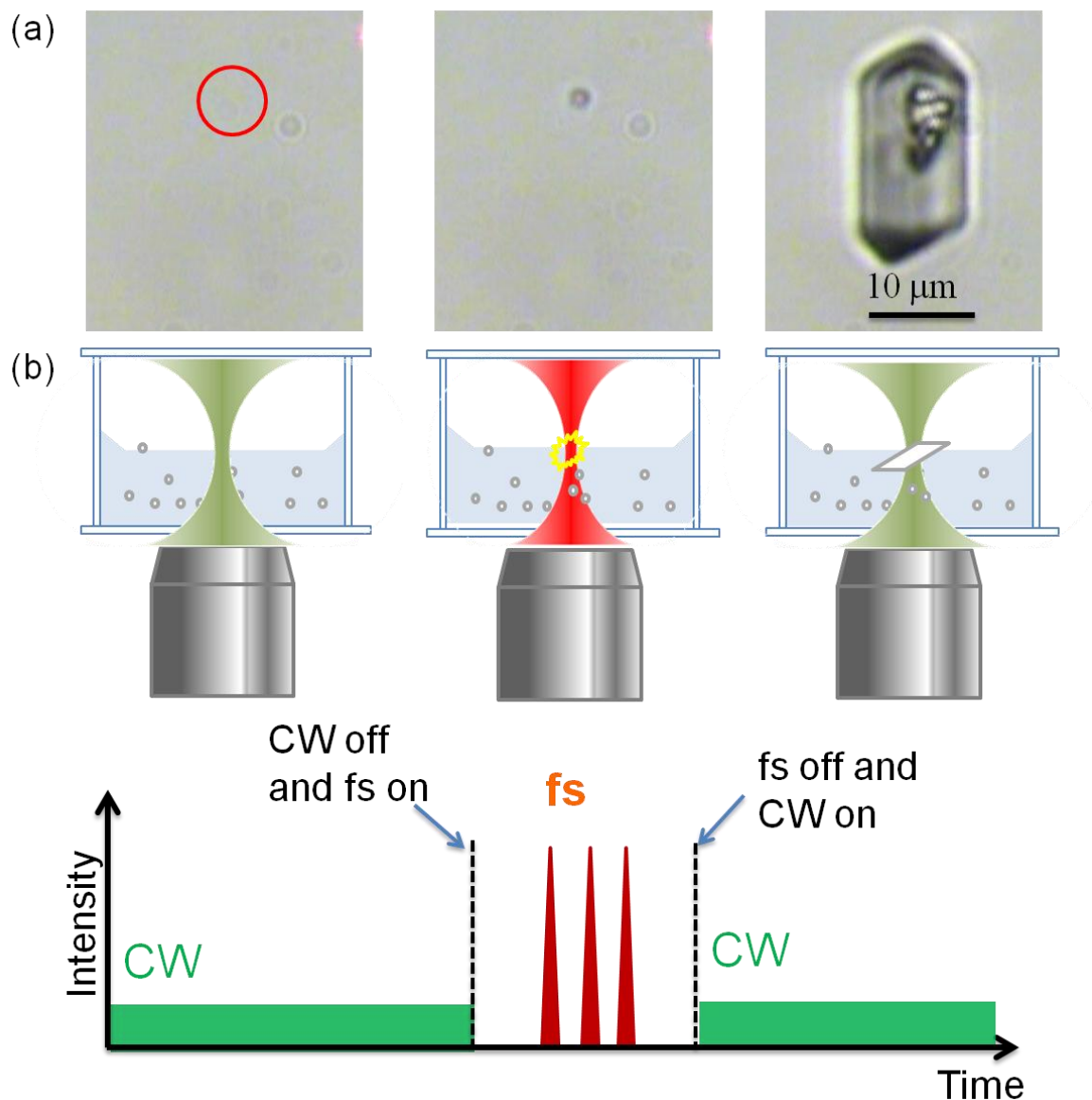


Fig. 5.11 (a) Images and (b) schematic drawing of temporally controlled laser-induced crystallization by millisecond short time irradiation of fs laser. Power of fs and CW lasers are 200 and 400 mW, respectively. Saturation degree of solution is 1.0 SS.

Here we consider possible mechanism of millisecond short time irradiation of fs laser-induced crystallization as shown in Fig 5.12. Initially a focused CW laser was collecting glycine clusters. At this moment we irradiated a millisecond short time of fs laser,

a small singular crystal was formed immediately.

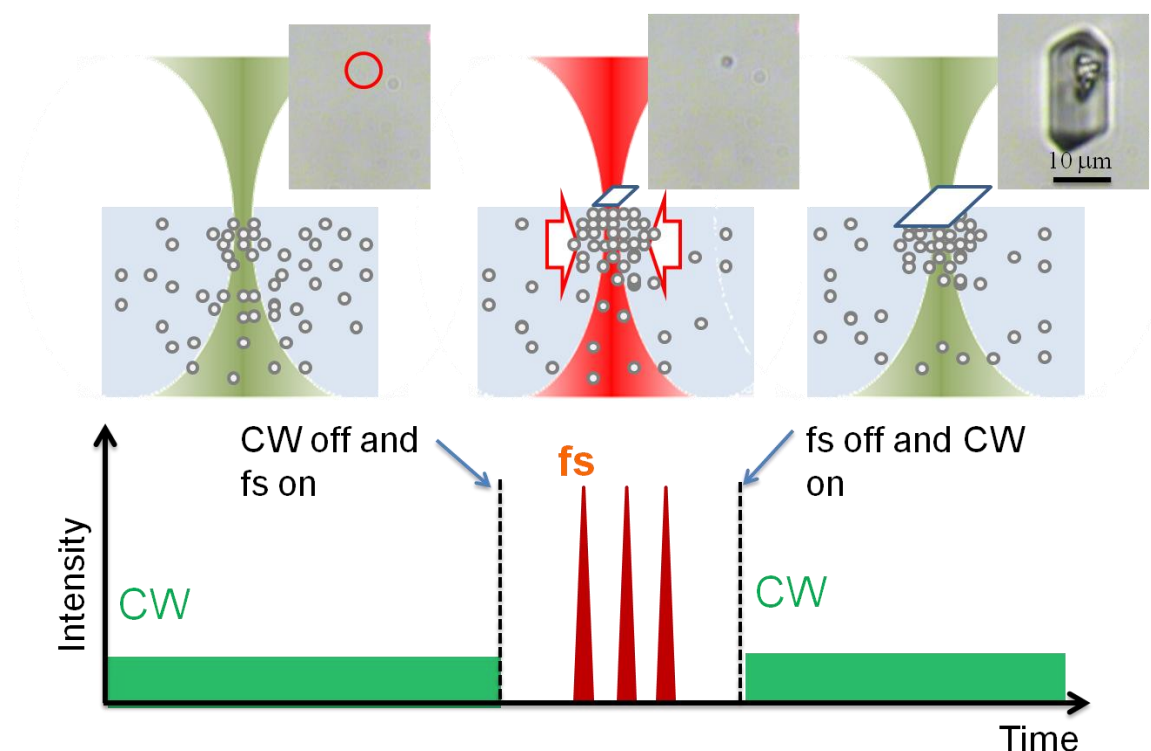


Fig. 5.12 Schematic mechanism of millisecond short time irradiation of fs laser induced crystallization. fs laser irradiation gathers the surrounding glycine cluster together. Suddenly concentration became high enough for crystallization.

We had discussed the trapping efficiency between fs and CW laser in chapter 4. Compare the photon number between fs and CW laser in short time range, higher optical trapping efficiency of pulsed laser can be attributed to the difference of the number of photons between fs ($\sim 10^{23}$) and CW ($\sim 10^{18}$) laser. In the case of Rayleigh dielectric particles trapping, the laser pulses can confine a larger number of the particles around the focal spot [67] which indicates a stronger trapping force exerted by fs laser. If we consider that conventional crystallization theory, CW laser induced local high concentration is correlated with

metastable concentration zone in the phase diagram shown in Fig.5.13. Following fs laser irradiation to induced high concentration area initiates sudden elevation of concentration by gathering surrounding glycine cluster into the focal point and very local highly saturated condition in the labile region are produced. Concentration at the focal point reached to the critical concentration for nucleation and eventually crystal was generated from the focal spot.

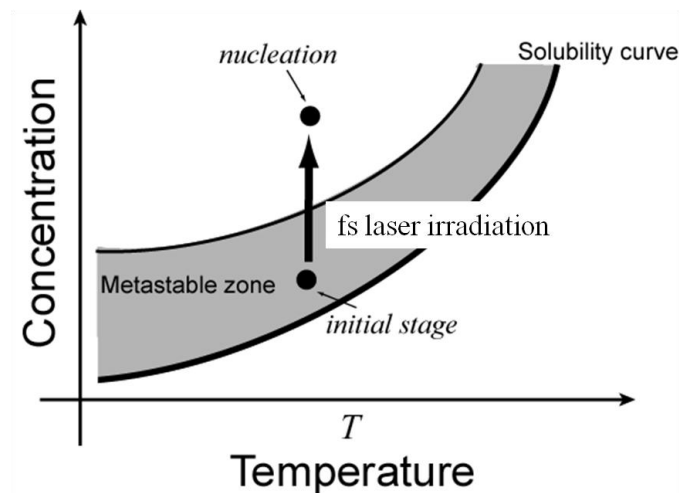


Fig. 5.13 Phase diagram showing the solubility depends on temperature and concentration. Suddenly fs laser irradiation induced highly saturated area in the labile region and finally persuaded nucleation and crystallization.

An advantage of this experiment is temporal controllability of crystallization timing. The advantage of laser trapping crystallization is spatial controllability of crystallization; crystallization always occur from the focal point of trapping laser. But the timing of

crystallization is random and we cannot control its timing. Laser trapping crystallization is stochastic phenomenon as well as conventional crystallization and fundamentally impossible to determine crystallization timing very precisely. We cannot make sure when crystallization will occur. However, with the combination of fs and CW laser, we can induce crystallization by fs laser after the local high concentration area preparation. This result implies that timing controlled crystallization with tight focusing of fs laser to metastable highly saturated condition can be possible. Our demonstration suggests that combination of fs and CW laser has further improved the laser trapping crystallization. Now we can prepare one singular crystal with not only having a spatially controllability but also temporal controllability by proposed method.



5.5 FTIR measurements for generated glycine crystals

Fabricated single crystal was examined by Fourier transform infrared (FTIR) measurement. By measuring the FTIR spectrum of each large crystal, we obtained two types of spectra. No mixture of α - and γ -polymorph spectra was observed. D_2O was used as a solvent to prevent thermal effect during laser irradiation ($\lambda = 1064$ nm). The acidic hydrogen atoms of an amino group of glycine in D_2O solution were deuterated. So the vibrational frequencies of *N*-deuterated glycine ($ND_3^+CH_2COO^-$, glycine- d_3) are important.

One of the spectra was fitted to α -form of *N*-deuterated glycine. The reported FTIR

spectrum of α -form showed the sharp peaks of CH_2 stretching around $3151\text{-}2971\text{ cm}^{-1}$, and the peaks of ND_3 deformation and rocking around $1180\text{-}1165$, and $828\text{-}762\text{ cm}^{-1}$, respectively [54, 68]. Characteristic peak values observed in the spectrum are summarized in table 5.14. All of these characteristic signals of the crystal we obtained are consistent with the previous reports. It is indicated that glycine was changed into glycine- d_3 in D_2O , and its polymorph was ascribed to the α -form. Another type of spectrum was fitted to γ -form of *N*-deuterated glycine. Typical spectral characteristic peaks of the γ -form of glycine- d_3 are the sharp peaks of CH_2 stretching at $3094\text{-}2971$, ND_3 deformation at $1167\text{-}1153$, and ND_3 rocking at $824\text{-}787\text{ cm}^{-1}$. These peaks are observed on the obtained spectrum. We can see the obvious difference of the peaks of α - and γ -form around $3151\text{-}2971$ and $3094\text{-}2971\text{ cm}^{-1}$, respectively. α -form usually shows two strong peaks around 3000 cm^{-1} , meanwhile a single strong peak at 2971 cm^{-1} observed for γ -form. These characteristic peaks can be used to distinguish the polymorph of *N*-deuterated glycine crystal.

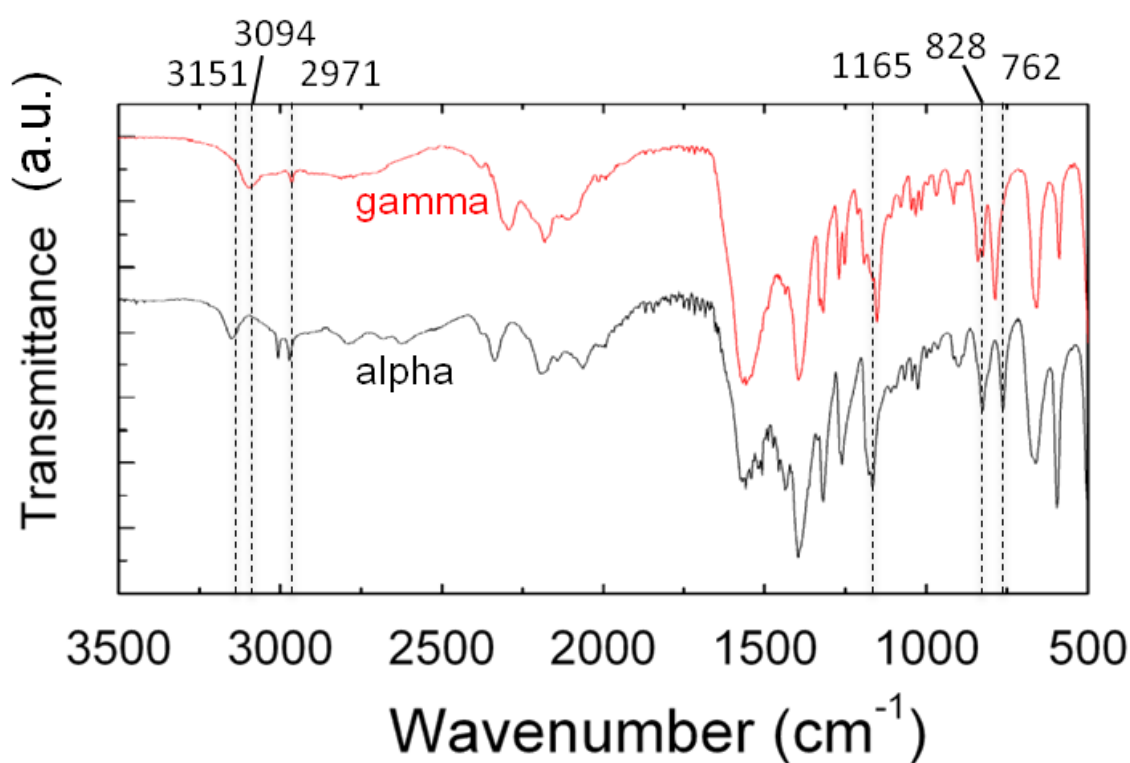


Fig. 5.14 FTIR spectra of glycine crystals prepared by single crystal formation by combination of CW and fs laser. α - and γ -form spectra of glycine- d_3 was obtained



Table 5.2 Vibrational frequencies of *N*-deuterated glycine ($\text{ND}_3^+\text{CH}_2\text{COO}^-$, glycine- d_3)

[3, 4].

| Vibration mode | α -polymorph | γ -polymorph |
|--|---------------------|---------------------|
| CH_2 stretching (cm^{-1}) | 3151-2971 | 3094-2971 |
| ND_3 deformation (cm^{-1}) | 1180-1165 | 1167-1153 |
| ND_3 rocking (cm^{-1}) | 828-762 | 824-787 |

By measuring FTIR, it was revealed that only α - and γ -polymorph *N*-deuterated glycine crystals were obtained from single crystal formation by a combination of fs and CW lasers.

α -polymorph crystal was dominant product. γ -polymorph crystal is the most stable thermodynamically among three polymorphs of glycine, but spontaneous crystallization almost gives kinetically stable α -polymorph under moderate experimental condition. Crystal of γ -polymorph is preferentially obtained under relatively severe conditions such as using acid and base aqueous solution [62]. β -polymorph glycine crystal was not obtained in this experiment. Laser trapping-induced molecular assembly provided a high concentration area for crystallization, this condition is more suitable for α - and γ -polymorph glycine crystal generation.

5.6 Summary

We have succeeded to improve the fs laser trapping crystallization method to make single crystal formation possible. Although fs laser trapping crystallization can generate crystal with higher probability and shorter crystallization time, this method cause laser ablation of generated crystal and frequently resulted in a polycrystal formation. We have demonstrated single crystal formation by combining fs and CW laser in this chapter. We demonstrated several different types of single crystal formation approach and showed all approach can form single crystal successfully. By measuring the FTIR spectrum of fabricated large crystal, we confirmed α - and γ -form glycine crystals were obtained and α -polymorph is dominant product.

Among examined approach for singular single crystal generation by direct utilization of fs laser for crystallization, millisecond fs laser irradiation to the locally induced high concentration region was most successful. We could obtain single crystal by very short time irradiation of fs laser. This method can form single crystal within a few to few tens of seconds after fs laser irradiation. It gives us not only spatial controllability of crystal generation but also high temporal controllability. We could obtain one large single crystal by applying demonstrated methods with high crystallization and success probability.

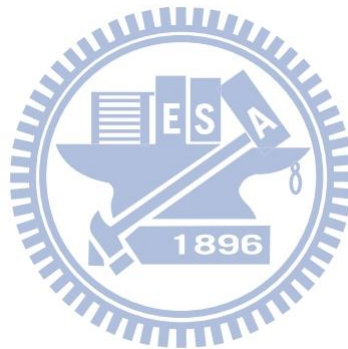


6. Summary

We first demonstrated low energy femtosecond laser utilized laser trapping crystallization of glycine without cavity bubble generation. fs laser-induced crystallization showed higher probability and shorter crystallization time than CW laser in the examined power range. Focused fs laser can induced crystallization with relatively low average power compared to CW laser. Examined power in fs laser trapping crystallization trials is too low to induce nonlinear phenomena such as breakdown of water, however, high energy of single pulse make generated crystal polycrystal due to the laser ablation occurred at the crystal surface. The mechanisms between amplified fs laser- and low energy fs laser-induced crystallization are different. Observed crystallization is due to the photon pressure of tightly focused fs laser and we think local high concentration induced by laser trapping of clusters by fs laser can explain the crystallization more reasonably. Higher optical trapping efficiency of pulsed laser than that of CW laser can be attributed to the difference of the number of photons between fs and CW, and effective crystallization by fs laser trapping.

To overcome a problem of polycrystal formation due to the ablation of crystal, we combined fs and CW laser trapping method. Controlling of irradiation timing of both lasers enables to make singular single crystal. Structural analysis indicates formed crystals are conventional glycine crystal where α -polymorph crystal is dominant product.

Most important achievement in this research is finding of spatiotemporally controlled single crystal generation method. We can trigger crystallization by applying fs laser just only for a short time to the locally induced high concentration region. Achieved second scale temporal controllability is unconventionally high for crystal generation method and can offer new methodology to study very initial process of crystallization with combining this method and high-resolution microscope imaging, micro spectroscopy and structural analysis methods such as X-ray diffraction. We can expect further understanding of crystallization dynamics and mechanism by introducing our method for extended research.



7. Reference

1. Ashkin, A., Acceleration and Trapping of Particles by Radiation Pressure. *Physical Review Letters* **1970**, *24* (4), 156-159.
2. Ashkin, A.; Gordon, J.P., Stability of radiation-pressure particle traps: an optical Earnshaw theorem. *Optics Letters* **1983**, *8* (10), 511-513.
3. Ashkin, A.; Dziedzic, J.M.; Bjorkholm, J.E.; Chu, S., Observation of a single-beam gradient force optical trap for dielectric particles. *Optics Letters* **1986**, *11* (5), 288-290.
4. Ashkin, A.; Dziedzic, J.M.; Yamane, T., Optical trapping and manipulation of single cells using infrared laser beams. *Nature* **1987**, *330* (6150), 769-771.
5. Chu, S.; Bjorkholm, J.E.; Ashkin, A.; Cable, A., Experimental Observation of Optically Trapped Atoms. *Physical Review Letters* **1986**, *57* (3), 314-317.
6. Dijk, M.A.v.; Kapitein, L.C.; Mameren, J.v.; Schmidt, C.F.; Peterman, E.J.G., Combining Optical Trapping and Single-Molecule Fluorescence Spectroscopy: Enhanced Photobleaching of Fluorophores. *Journal of Physical Chemistry B* **2004**, *108* (20), 6479-6484.
7. Neuman, K.C.; Block, S.M., Optical trapping. *REVIEW OF SCIENTIFIC INSTRUMENTS* **2004**, *75*, 2787-2809.
8. Sasaki, K.; Koshioka, M.; Misawa, H.; Kitamura, N.; Masuhara, H., Optical trapping of a metal article and a water droplet by a scanning laser beam. *Applied Physics Letters* **1991**, *60*, 807-809.
9. Crocker, J.C.; Grier, D.G., When Like Charges Attract: The Effects of Geometrical Confinement on Long-Range Colloidal Interactions. *Physical Review Letters* **1996**, *77*, 1897-1900.
10. Bar-Ziv, R.; Moses, E., Instability and "Pearling" States Produced in Tubular Membranes by Competition of Curvature and Tension. *Physical Review Letters* **1994**, *73*, 1392-1395.
11. C, S.; Chapin; Germain, V.; Dufresne, E.R., Automated trapping, assembly, and sorting with holographic optical tweezers. *Optics Express* **2006**, *14*, 13095-13110.
12. Hofkens, J.; Hotta, J.; Sasaki, K.; Masuhara, H.; Iwai, K., Molecular Assembling by the Radiation Pressure of a Focused Laser Beam: Poly(N-isopropylacrylamide) in Aqueous Solution. *Langmuir* **1997**, *13* (3), 414-419.
13. Borowicz, P.; Hotta, J.-i.; Sasaki, K.; Masuhara, H., Chemical and Optical Mechanism of Microparticle Formation of Poly(N-vinylcarbazole) in N,N-Dimethylformamide by Photon Pressure of a Focused Near-Infrared Laser Beam. *The Journal of Physical Chemistry B* **1998**, *102*, 1896-1901.
14. Hotta, J.-i.; Sasaki, K.; Masuhara, H., Laser-Controlled Assembling of Repulsive Unimolecular Micelles in Aqueous Solution. *The Journal of Physical Chemistry B* **1998**,

- 102, 7687-7690.
15. Smith, T.A.; Hotta, J.-i.; Sasaki, K.; Masuhara, H.; Itoh, Y., Photon Pressure-Induced Association of Nanometer-Sized Polymer Chains in Solution. *The Journal of Physical Chemistry B* **1999**, *103*, 1160-1163.
 16. Borowicz, P.; Hotta, J.-i.; Sasaki, K.; Masuhara, H., Laser-Controlled Association of Poly(N-vinylcarbazole) in Organic Solvents: Radiation Pressure Effect of a Focused Near-Infrared Laser Beam. *The Journal of Physical Chemistry B* **1997**, *101*, 5900-5904.
 17. Gugliotti, M.; Baptista, M.S.; Politi, M.J., Laser-Induced Marangoni Convection in the Presence of Surfactant Monolayers. *Langmuir* **2002**, *18*, 9792-9798.
 18. Mao, Z.-S.; Chen, J., Numerical simulation of the Marangoni effect on mass transfer to single slowly moving drops in the liquid-liquid system. *Chemical Engineering Science* **2004**, *59* (8-9), 1815-1828.
 19. Louchev, O.A.; Juodkazis, S.; Murazawa, N.; Wada, S.; Misawa, H., Coupled laser molecular trapping, cluster assembly, and deposition fed by laser-induced Marangoni convection. *Optics Express* **2008**, *16*, 5673-5680.
 20. Uwada, T.; Sugiyama, T.; Miura, A.; Masuhara, H., Wide-field light scattering imaging of laser trapping dynamics of single gold nanoparticles in solution. **2010**, 77620N-77620N-8.
 21. Tsuboi, Y.; Shoji, T.; Kitamura, N., Optical Trapping of Amino Acids in Aqueous Solutions. *The Journal of Physical Chemistry C* **2010**, *114*, 5589-5593.
 22. Tsuboi, Y.; Shoji, T.; Kitamura, N., Crystallization of Lysozyme Based on Molecular Assembling by Photon Pressure. *Japanese Journal of Applied Physics* **2007**, *114*, L1234-L1236.
 23. Singer, W.; Gibson, U.J.; Nieminen, T.A.; Heckenberg, N.R.; Rubinsztein-Dunlop, H., Towards Crystallization using Optical Tweezers. *Proc. of SPIE* **2006**, *6038*, 60380B-1~8.
 24. Singer, W.; Nieminen, T.A.; Gibson, U.J.; Heckenberg, N.R.; Rubinsztein-Dunlop, H., Orientation of optically trapped nonspherical birefringent particles. *Physical Review* **2006**, *73*, 1-5.
 25. Singer, W.; Rubinsztein-Dunlop, H.; Gibson, U., Manipulation and growth of birefringent protein crystals in optical tweezers. *Optics Express* **2004**, *12*, 6440-6445.
 26. Malmqvist, L.; Hertz, H.M., Second-harmonic generation in optically trapped nonlinear particles with pulsed lasers. *Applied Optics* **1995**, *34* (18), 3392-3397.
 27. Xing, Q.; Mao, F.; Chai, L.; Wang, Q., Numerical modeling and theoretical analysis of femtosecond laser tweezers. *Optics & Laser Technology* **2004**, *36* (8), 635-639.
 28. Agate, B.; Brown, C.; Sibbett, W.; Dholakia, K., Femtosecond optical tweezers for in-situ control of two-photon fluorescence. *Optics Express* **2004**, *12* (13), 3011-3017.
 29. Pan, L.; Ishikawa, A.; Tamai, N., Detection of optical trapping of CdTe quantum dots by two-photon-induced luminescence. *Physical Review B* **2007**, *75* (16), 161305.
 30. Jiang, Y.; Narushima, T.; Okamoto, H., Nonlinear optical effects in trapping nanoparticles

- with femtosecond pulses. *Nature Physics* **2010**, 6 (12), 1005-1009.
31. McPherson, A., *Crystallization of biological macromolecules*. Cold Spring Harbor Laboratory Press: New York, USA 1999.
 32. Hünefeld, F.L., *Der Chemismus in der thierischen Organisation* **1840**, 158-163.
 33. Hodgkin, D.C.; Kamper, J.; Lindsay, J.; MacKay, M.; Pickworth, J.; Robertson, J.H.; Shoemaker, C.B.; White, J.G.; Prosen, R.J.; Trueblood, K.N., The Structure of Vitamin B12 I. An Outline of the Crystallographic Investigation of Vitamin B12. *Proc. R. Soc. Lond. A* **1957**, 242, 228-263.
 34. Vekilov, P.G., Nucleation. *Crystal Growth & Design* **2010**, 10 (12), 5007-5019.
 35. Vekilov, P.G., Dense Liquid Precursor for the Nucleation of Ordered Solid Phases from Solution. *Crystal Growth & Design* **2004**, 4, 671-685.
 36. Erdemir, D.; Lee, A.Y.; Myerson, A.S., Nucleation of Crystals from Solution: Classical and Two-Step Models. *Accounts of Chemical Research* **2009**, 42 (5), 621-629.
 37. Garetz, B.A.; Aber, J.E.; Goddard, N.L.; Young, R.G.; Myerson, A.S., Nonphotochemical, Polarization-Dependent, Laser-Induced Nucleation in Supersaturated Aqueous Urea Solutions. *Physical Review Letters* **1996**, 77 (16), 3475-3476.
 38. Garetz, B.A.; Matic, J.; Myerson, A.S., Polarization Switching of Crystal Structure in the Nonphotochemical Light-Induced Nucleation of Supersaturated Aqueous Glycine Solutions. *Physical Review Letters* **2002**, 89 (17), 175501.
 39. Sun, X.; Garetz, B.A.; Myerson, A.S., Supersaturation and Polarization Dependence of Polymorph Control in the Nonphotochemical Laser-Induced Nucleation (NPLIN) of Aqueous Glycine Solutions. *Crystal Growth & Design* **2006**, 6 (3), 684-689.
 40. Aber, J.E.; Arnold, S.; Garetz, B.A.; Myerson, A.S., Strong dc Electric Field Applied to Supersaturated Aqueous Glycine Solution Induces Nucleation of the gamma Polymorph. *Physical Review Letters* **2005**, 94 (14), 145503.
 41. Okutsu, T.; Isomura, K.; Kakinuma, N.; Horiuchi, H.; Unno, M.; Matsumoto, H.; Hiratsuka, H., Laser-Induced Morphology Control and Epitaxy of Dipara-anthracene Produced from the Photochemical Reaction of Anthracene. *Crystal Growth & Design* **2004**, 5 (2), 461-465.
 42. Okutsu, T.; Furuta, K.; Terao, M.; Hiratsuka, H.; Yamano, A.; Ferte, N.; Veessler, S., Light-Induced Nucleation of Metastable Hen Egg-White Lysozyme Solutions. *Crystal Growth & Design* **2005**, 5 (4), 1393-1398.
 43. Okutsu, T.; Sugiyama, K.; Furuta, K.; Watanebe, I.; Mori, H.; Obi, K.; Horota, K.; Horiuchi, H.; Sazaki, G.; Veessler, S.; Hiratsuka, H., Photochemically induced nucleation in supersaturated and undersaturated thaumatin solutions. *Journal of Photochemistry and Photobiology A: Chemistry* **2007**, 190 (1), 88-93.
 44. Furuta, K.; Horiuchi, H.; Hiratsuka, H.; Okutsu, T., Photochemically Induced Nucleation of Ribonuclease A Enhanced by a Stable Protein Dimer Produced from the Photochemical

- Reaction of Tyr Residual Groups. *Crystal Growth & Design* **2008**, *8* (6), 1886-1889.
45. Adachi, H.; Takano, K.; Hosokawa, Y.; Inoue, T.; Mori, Y.; Matsumura, H.; Yoshimura, M.; Tsunaka, Y.; Morikawa, M.; Kanaya, S.; Masuhara, H.; Kai, Y.; Sasaki, T., Laser Irradiated Growth of Protein Crystal. *Jpn. J. Appl. Phys.* **2003**, *42* (Part 2, No. 7B), L798-800.
46. Yoshikawa, H.Y.; Hosokawa, Y.; Masuhara, H., Explosive Crystallization of Urea Triggered by Focused Femtosecond Laser Irradiation. *Jpn. J. Appl. Phys.* **2006**, *45* (1), L23-26.
47. Nakamura, K.; Hosokawa, Y.; Masuhara, H., Anthracene Crystallization Induced by Single-Shot Femtosecond Laser Irradiation: Experimental Evidence for the Important Role of Bubbles. *Cryst. Growth Des.* **2007**, *7* (5), 885-889.
48. Hosokawa, Y.; Adachi, H.; Yoshimura, M.; Mori, Y.; Sasaki, T.; Masuhara, H., Femtosecond Laser-Induced Crystallization of 4-(Dimethylamino)-N-methyl-4-stilbazolium Tosylate. *Cryst. Growth Des.* **2005**, *5* (3), 861-863.
49. Uwada, T., *Journal of Crystal Growth*, submitted. **2012**.
50. Murai, R.; Yoshikawa, H.Y.; Takahashi, Y.; Maruyama, M.; Sugiyama, S.; Sasaki, G.; Adachi, H.; Takano, K.; Matsumura, H.; Murakami, S.; Inoue, T.; Mori, Y., Enhancement of femtosecond laser-induced nucleation of protein in a gel solution. *Appl. Phys. Lett.* **2010**, *96* (4), 043702-3.
51. Sugiyama, T.; Adachi, T.; Masuhara, H., Crystallization of Glycine by Photon Pressure of a Focused CW Laser Beam. *Chemistry Letters* **2007**, *36* (12), 1480-1481.
52. Sugiyama, T.; Adachi, T.; Masuhara, H., Crystal Growth of Glycine Controlled by a Focused CW Near-infrared Laser Beam. *Chemistry Letters* **2009**, *38* (5), 482-483.
53. Rungsimanon, T.; Yuyama, K.-i.; Sugiyama, T.; Masuhara, H., Crystallization in Unsaturated Glycine/D₂O Solution Achieved by Irradiating a Focused Continuous Wave Near Infrared Laser. *Crystal Growth & Design* **2010**, *10* (11), 4686-4688.
54. Rungsimanon, T.; Yuyama, K.; Sugiyama, T.; Masuhara, H.; Tohnai, N.; Miyata, M., Control of Crystal Polymorph of Glycine by Photon Pressure of a Focused Continuous Wave Near-Infrared Laser Beam. *The Journal of Physical Chemistry Letters* **2010**, *1* (3), 599-603.
55. Yuyama, K.-i.; Sugiyama, T.; Masuhara, H., Millimeter-Scale Dense Liquid Droplet Formation and Crystallization in Glycine Solution Induced by Photon Pressure. *The Journal of Physical Chemistry Letters* **2010**, *1* (9), 1321-1325.
56. Chattopadhyay, S.; Erdemir, D.; Evans, J.M.B.; Ilavsky, J.; Amenitsch, H.; Segre, C.U.; Myerson, A.S., SAXS Study of the Nucleation of Glycine Crystals from a Supersaturated Solution. *Crystal Growth & Design* **2005**, *5* (2), 523-527.
57. Kuniyama, K.S., Crystal growth of γ -glycine. *Journal of Crystal Growth* **1974**, *23* (4), 351-352.

58. Albrecht, G.; Corey, R.B., The Crystal Structure of Glycine. *Journal of the American Chemical Society* **1939**, *61* (5), 1087-1103.
59. Boldyreve, E.V.; Drebuschak, V.A.; Drebuschak, T.N.; Paukov, I.E.; Kovalevskaya, Y.A.; Shutova, E.S., POLYMORPHISM OF GLYCINE Thermodynamics aspects. Part I. Relative stability of the polymorphs. *Journal of Thermal Analysis and Calorimetry* **2003**, *73*, 409-418.
60. Iitaka, Y., The Crystal Structure of γ -Glycine. *Acta Crystallographica* **1961**, *14*, 1-10.
61. Srinivasan, K., Crystal growth of α and γ glycine polymorphs and their polymorphic phase transformations. *Journal of Crystal Growth* **2008**, *311* (1), 156-162.
62. Bhat, M.N.; Dharmaprasath, S.M., Effect of solvents on the growth morphology and physical characteristics of nonlinear optical γ -glycine crystals. *Journal of Crystal Growth* **2002**, *242* (1-2), 245-252.
63. Yuyama, K.-i.; Rungsimanon, T.; Sugiyama, T.; Masuhara, H., Selective Fabrication of α - and γ -Polymorphs of Glycine by Intense Polarized Continuous Wave Laser Beams. *Crystal Growth & Design* **2012**, *12* (5), 2427-2434.
64. Ito, S.; Sugiyama, T.; Toitani, N.; Katayama, G.; Miyasaka, H., Application of Fluorescence Correlation Spectroscopy to the Measurement of Local Temperature in Solutions under Optical Trapping Condition. *The Journal of Physical Chemistry B* **2007**, *111* (9), 2365-2371.
65. Gendron, P.O.; Avaltroni, F.; Wilkinson, K., Diffusion Coefficients of Several Rhodamine Derivatives as Determined by Pulsed Field Gradient-Nuclear Magnetic Resonance and Fluorescence Correlation Spectroscopy. *Journal of Fluorescence* **2008**, *18* (6), 1093-1101.
66. Vogel, A.; Noack, J.; Hüttman, G.; Paltauf, G., Mechanisms of femtosecond laser nanosurgery of cells and tissues. *Applied Physics B: Lasers and Optics* **2005**, *81* (8), 1015-1047.
67. Usman, A.; Chiang, W.-Y.; Masuhara, H., Optical trapping and polarization-controlled scattering of dielectric spherical nanoparticles by femtosecond laser pulses. *Journal of Photochemistry and Photobiology A: Chemistry* **2012**, *234*, 83-90.
68. Suzuki, S.; Shimanouchi, T.; Tsuboi, M., Normal vibrations of glycine and deuterated glycine molecules. *Spectrochimica Acta* **1963**, *19* (7), 1195-1208.